Laser-Induced Breakdown Spectroscopy
(LIBS)

Content

- Introduction to fundamentals of LIBS
- Basic instrumentation and configurations
- Double pulse LIBS (instrumentation)
- Depth profiling (zinc coated steel, ceramic tiles)
- Elemental mapping (teeth, plants, urinary stones ...)

Content

- LIBS techniques for powder materials (pressed pellets)
- LIBS techniques for liquid samples (algae suspension)
- LIBS technique for nanoparticles (QDs)
- Remote analysis by LIBS (identification of biominerals)
- Conclusion

Laser beam - solid sample interaction

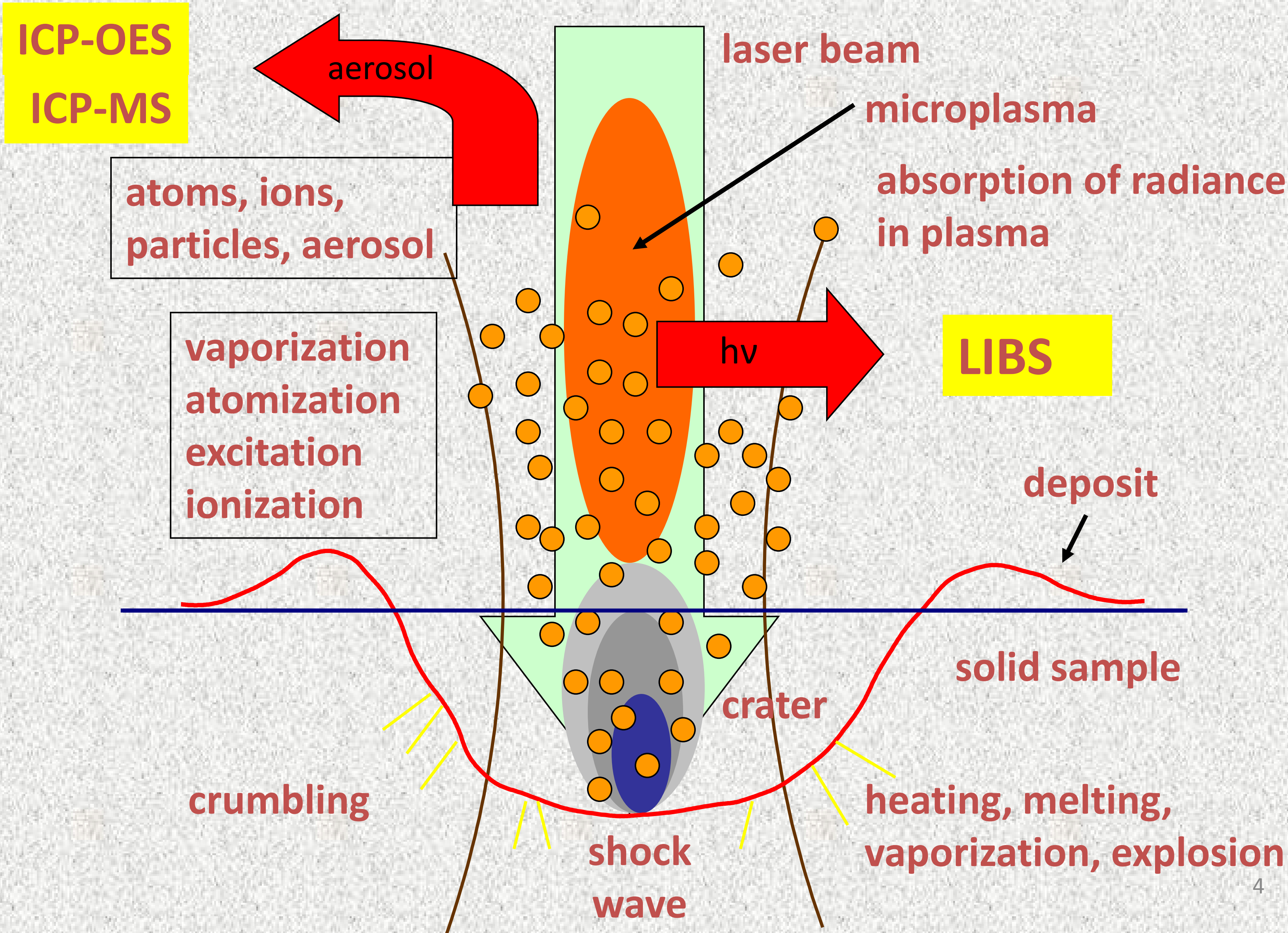

Laser beam - solid sample interaction

Plasma ignition: **ns laser ($10^7 – 10^{11}$ W/cm^2)**
fs laser ($10^{12} – 10^{17}$ W/cm^2)

Thermal vaporization ($10^{-9} – 10^{-8}$ s)
Non-thermal ablation ($10^{-9} – 10^{-8}$ s)
Plasma shielding ($10^{-9} – 10^{-8}$ s)

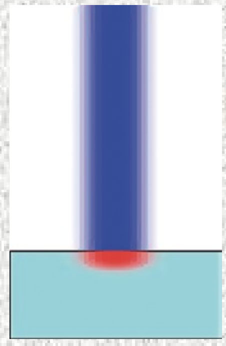

Plasma expansion and cooling:

Shockwave propagation
Plasma expansion ($10^{-11} – 10^{-6}$ s)
Plasma radiation cooling ($10^{-6} – 10^{-4}$ s)

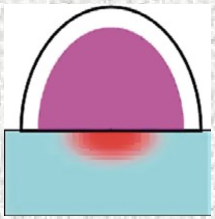

Particle ejection and condensation:

Ejection of liquid droplet ($10^{-8} – 10^{-6}$ s)
Solid exfoliation ($10^{-8} – 10^{-6}$ s)
Nano particles formation ($10^{-4} – 10^{-3}$ s)

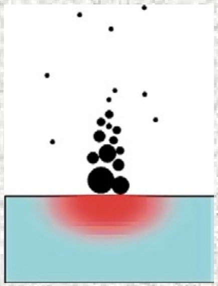

Important time periods after plasma formation

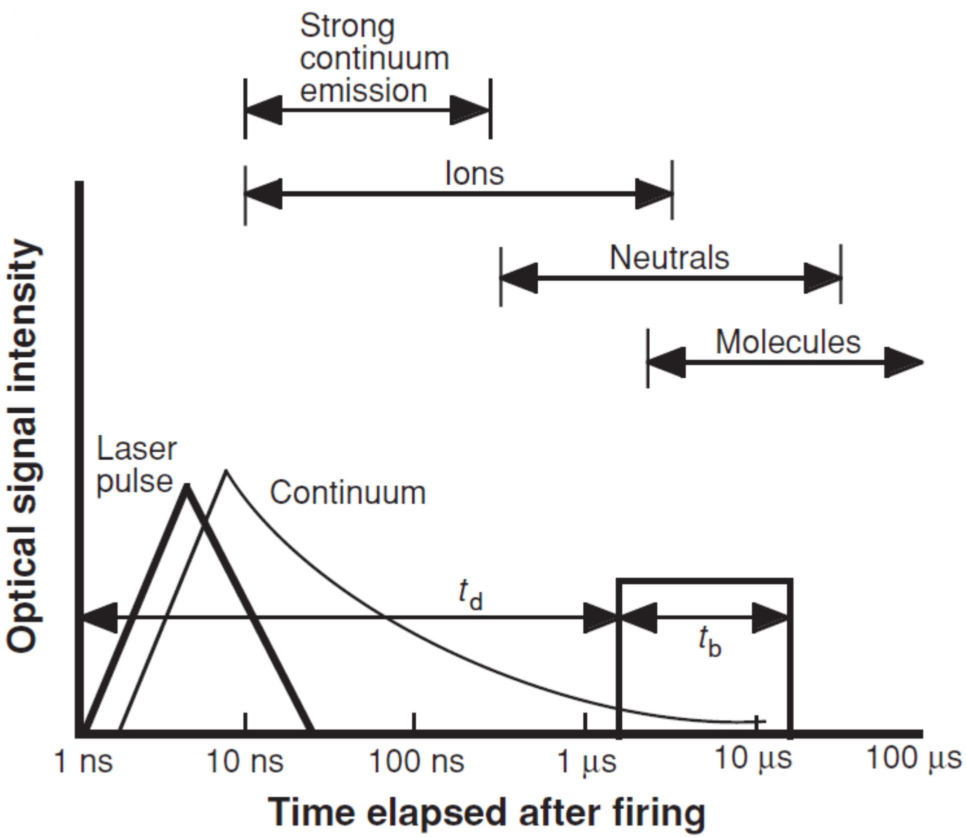

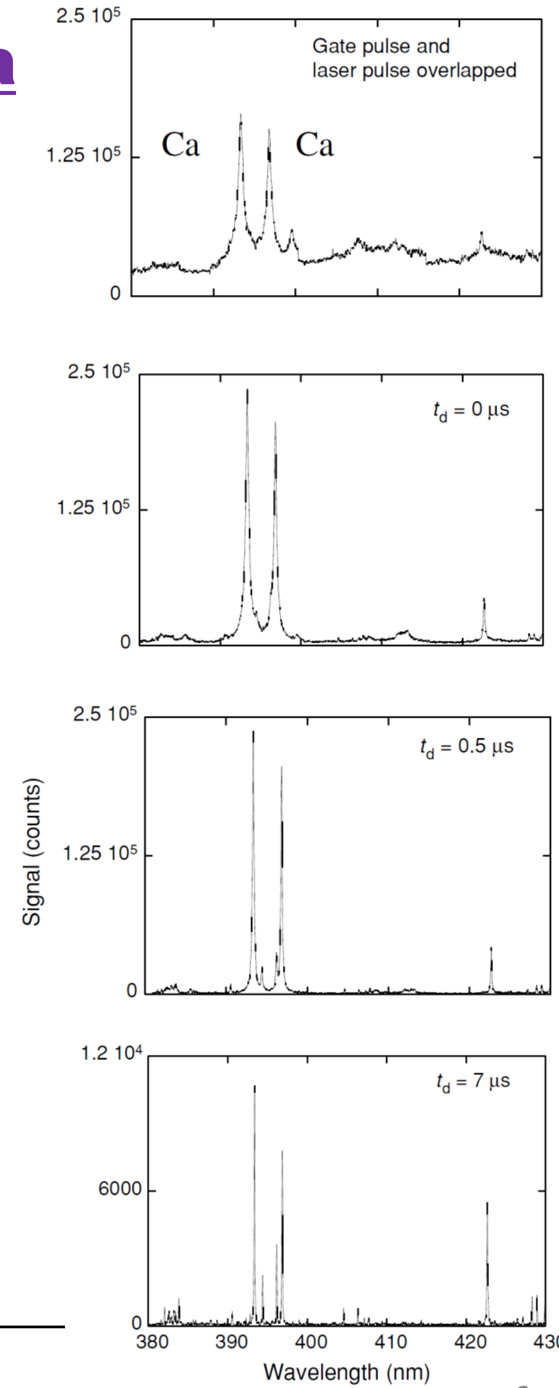

t_d - delay time, t_b – gate pulse width

Laser-Induced Breakdown Spectroscopy (LIBS), Fundamentals and Applications Andrzej W. Miziolek, Vincenzo Palleschi, Israel Schechter © *2006 Cambridge*

LIBS - lasers

Table 3.1 Specifications of lasers used for LIBS

Type	Wavelength (nm)	Pulse width (ns)	Rep. rate (Hz)	Comments related to LIBS applications
Nd:YAG (s)	Fundamental: 1064 Harmonics: 532, 355, 266	6–15 4–8	ss to 20	(1) Fundamental wavelength easily shifted to provide harmonic wavelengths (2) Available in very compact form for small instrumentation (3) Good beam quality possible (4) Dual-pulse capabilities in single unit (5) Flashlamp or diode-pumped available
Excimer (g)	XeCl: 308 KrF: 248 ArF: 194	20 ns	ss to 200	(1) Requires periodic change of gases (2) Beam quality less than Nd:YAG laser (3) Provides UV wavelengths only
CO_2 (g)	10 600	200 (with 1000 ns trailing edge)	ss to 200	(1) Requires periodic change of gases or gas flow (2) Does not couple well into many metals (3) Beam quality less than Nd:YAG laser
Microchip	1064	<1 ns	1–10 k	(1) Good mode and beam quality (2) High shot-to-shot pulse stability
Ti:sapphire: femtosecond (s)	~800 (Δλ ~ 10 nm)	20–200 fs	$10–10^3$	
Fiber laser (s)	Nd^{+3} 900 Pr^{+3} 1060 Er^{+3} 1540	<50	25–500 k	

Notes: (s) = solid state laser; (g) = gas laser; ss = single shot.

Handbook of Laser-Induced Breakdown Spectroscopy D. Cremers and L. Radziemski

Basic configurations

1. Experimental setup with pierced mirror

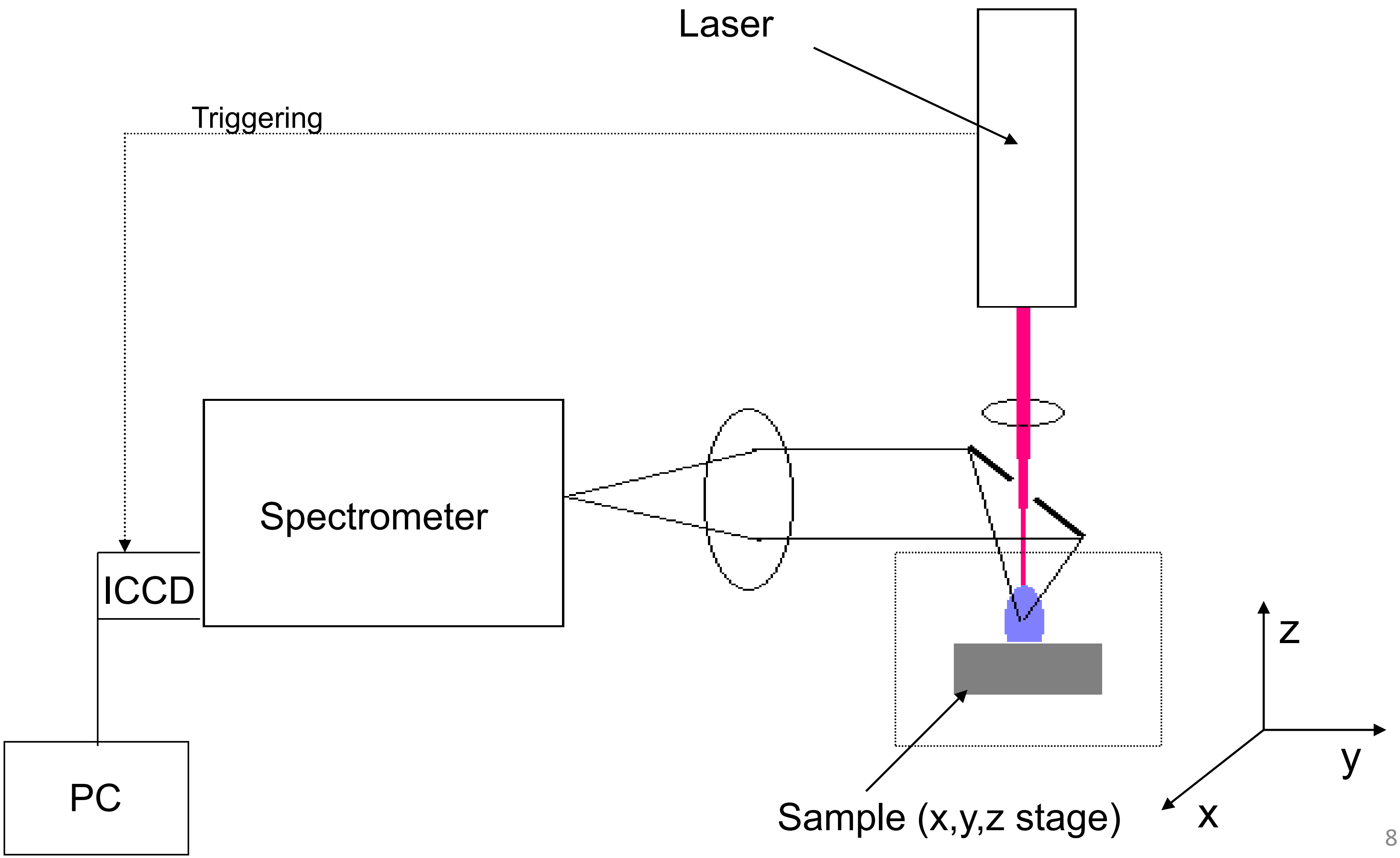

Basic configurations

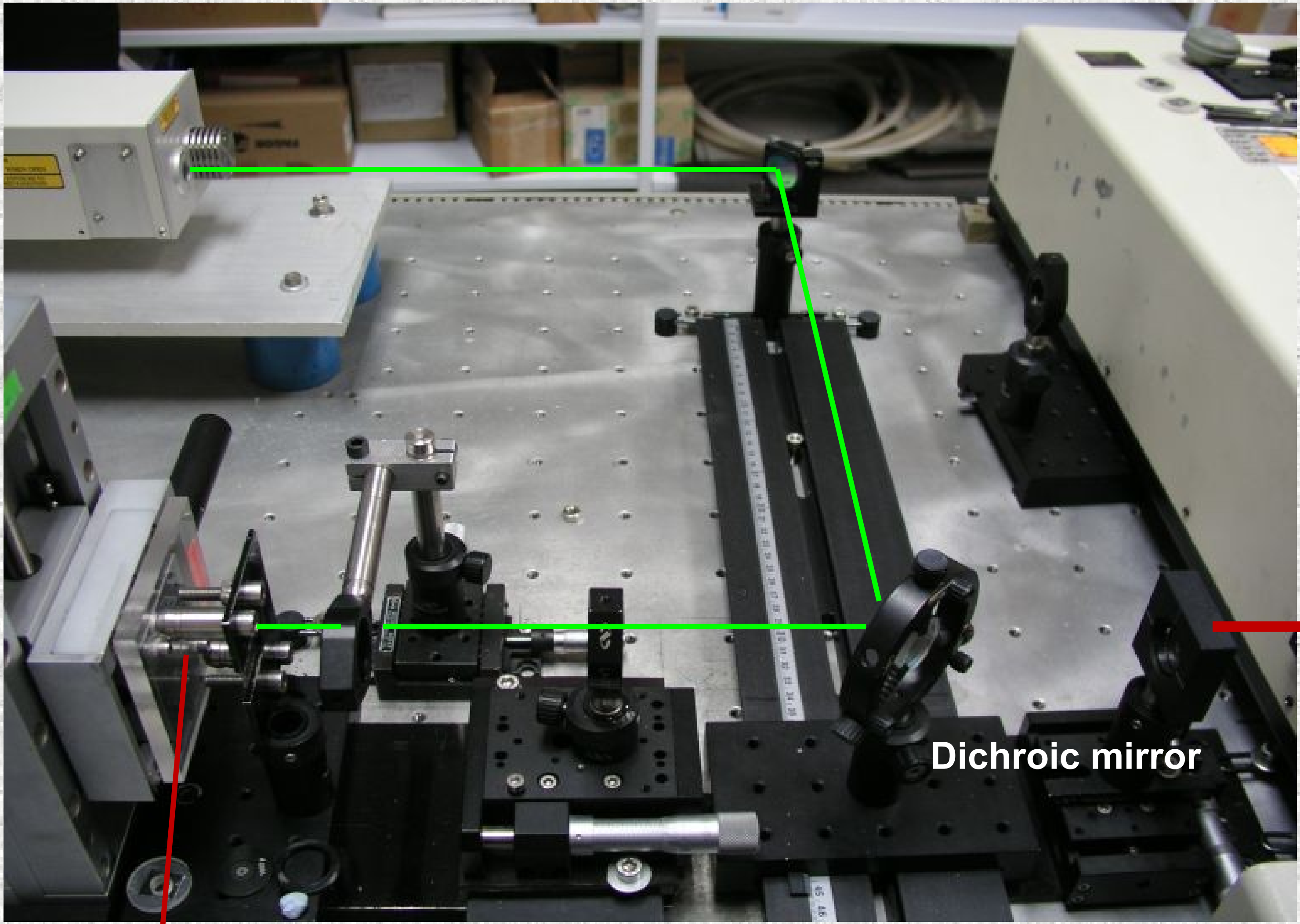

Basic configurations

2. Experimental setup with optical fiber

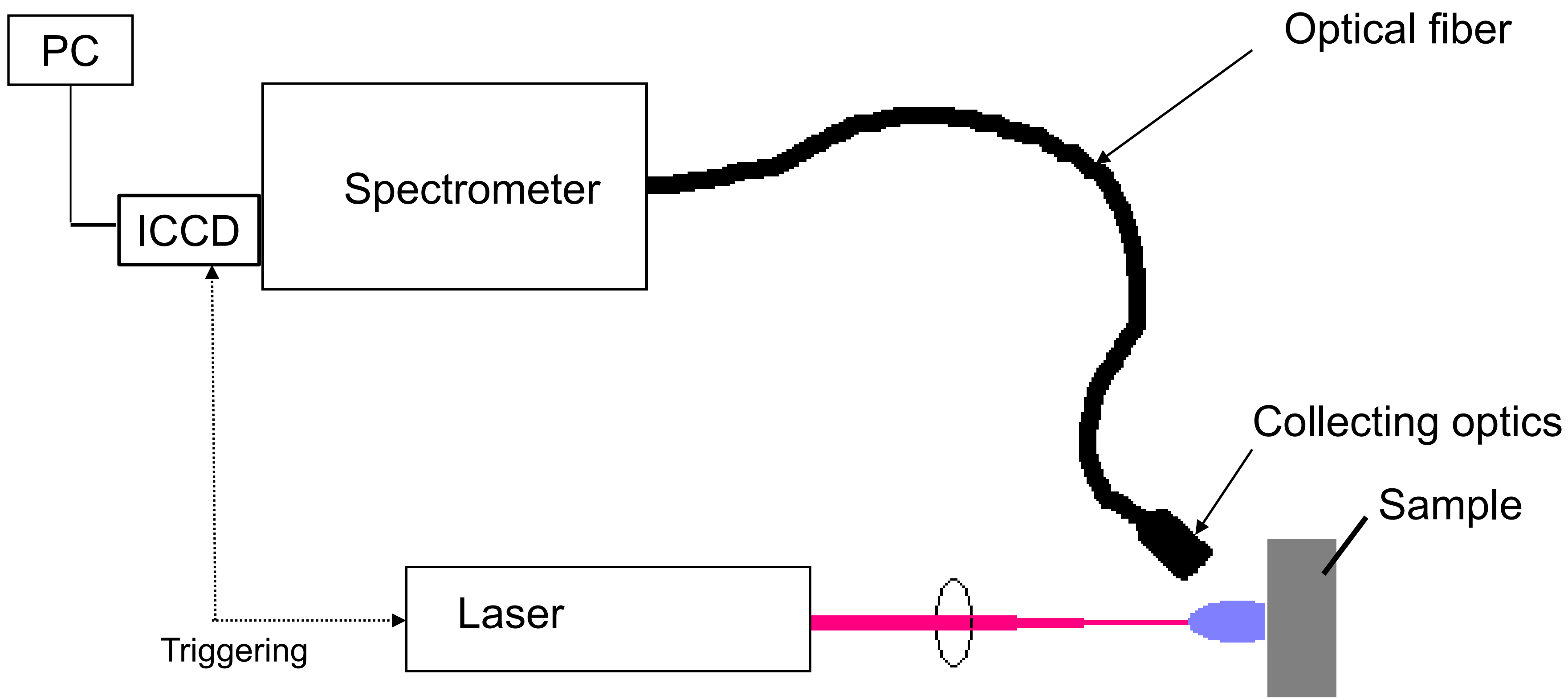

Basic configurations

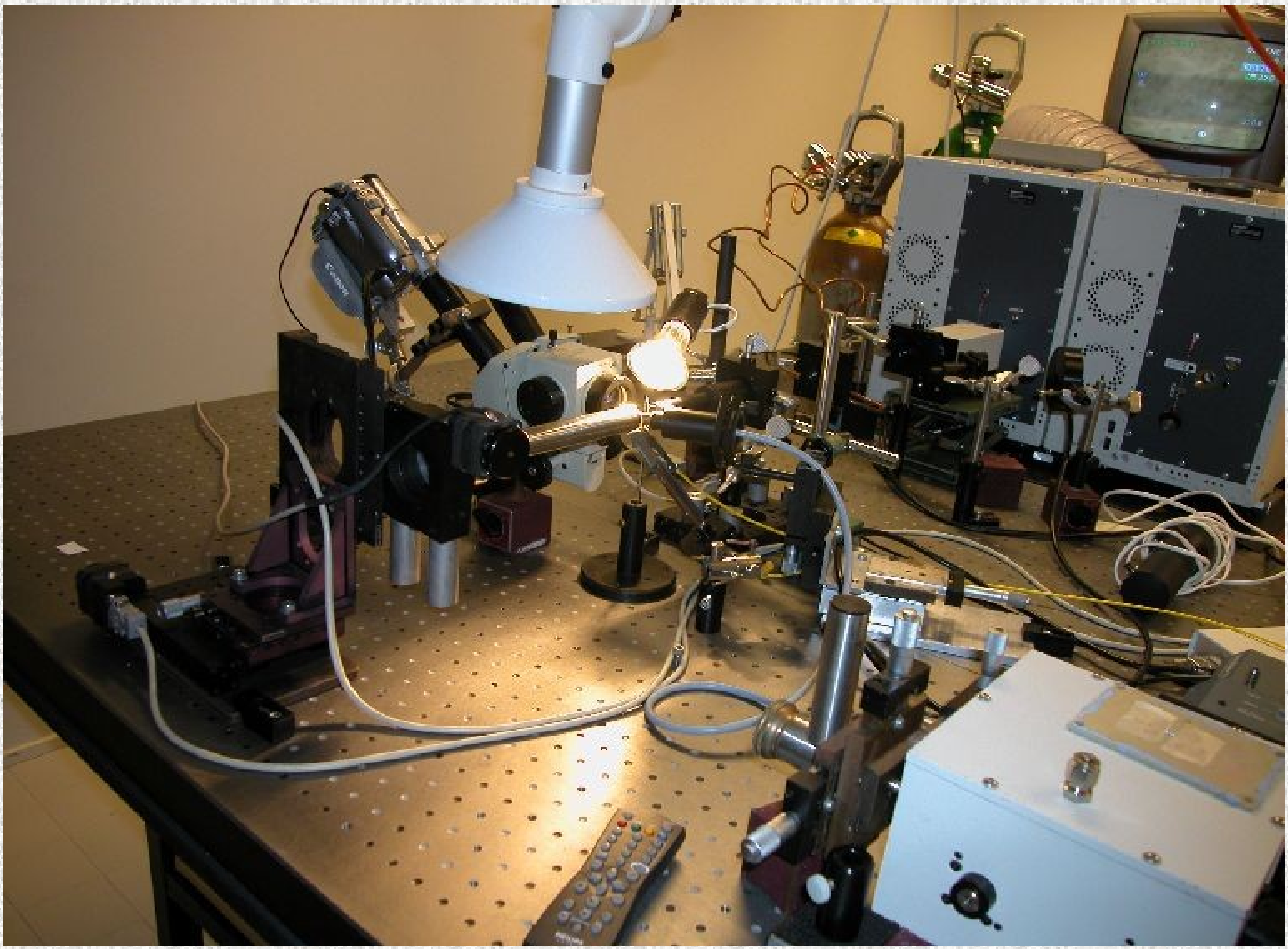

Basic configurations

3. Experimental setup with optical fiber

(portable LIBS, underwater measurements)

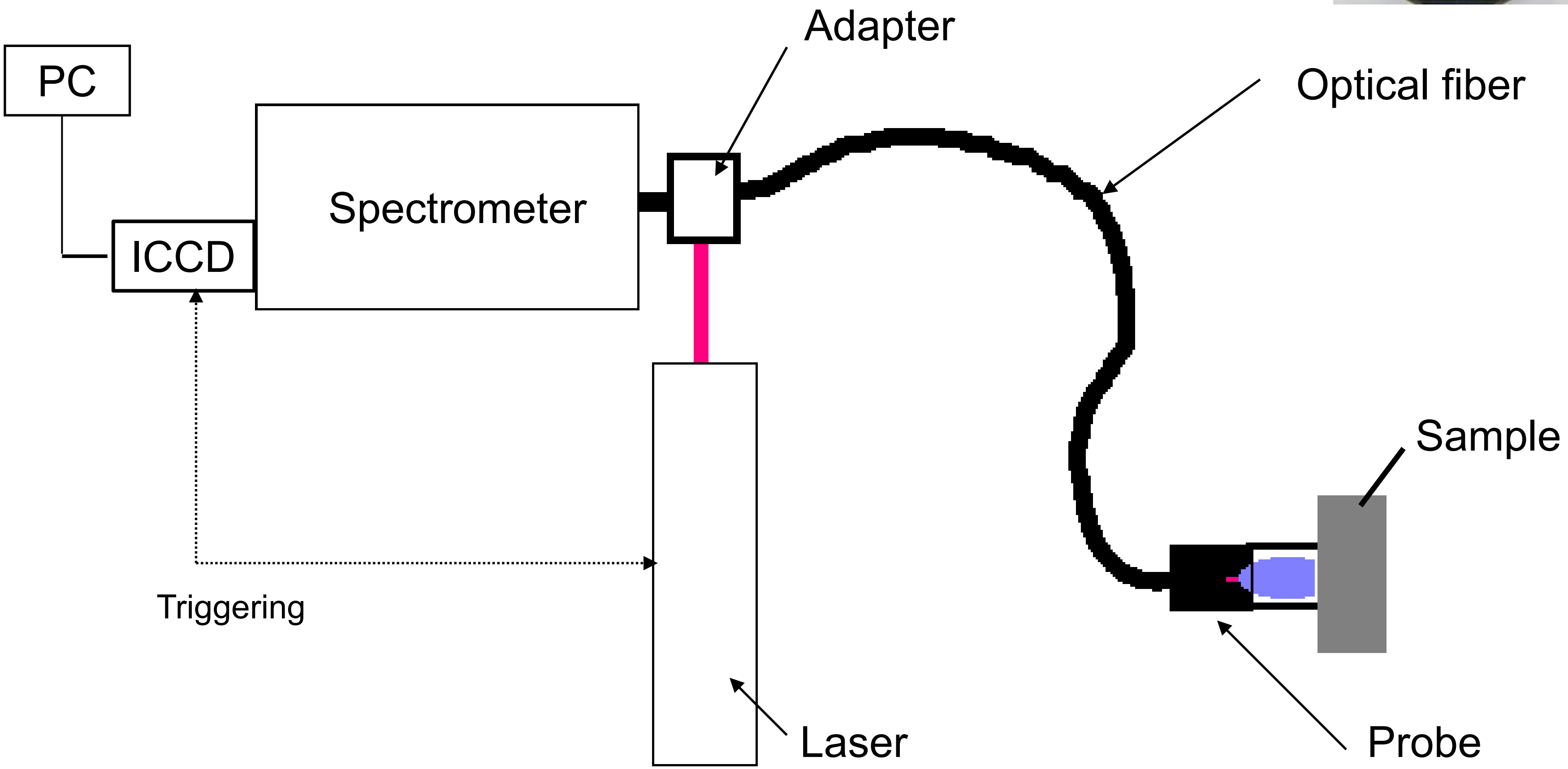

Basic configurations

3. Experimental setup with telescope

(Stand-off measurements)

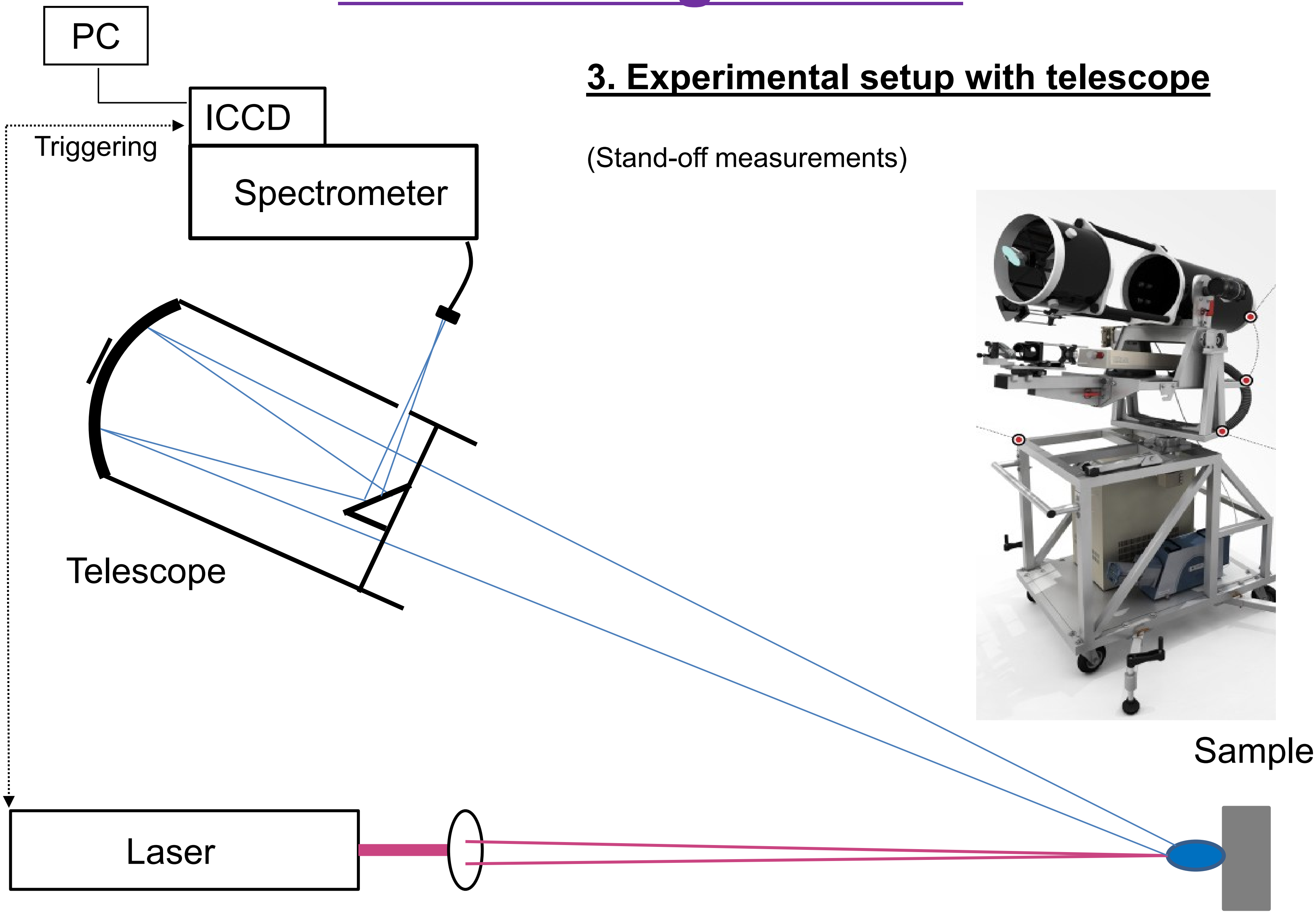

MU setup - 1st generation

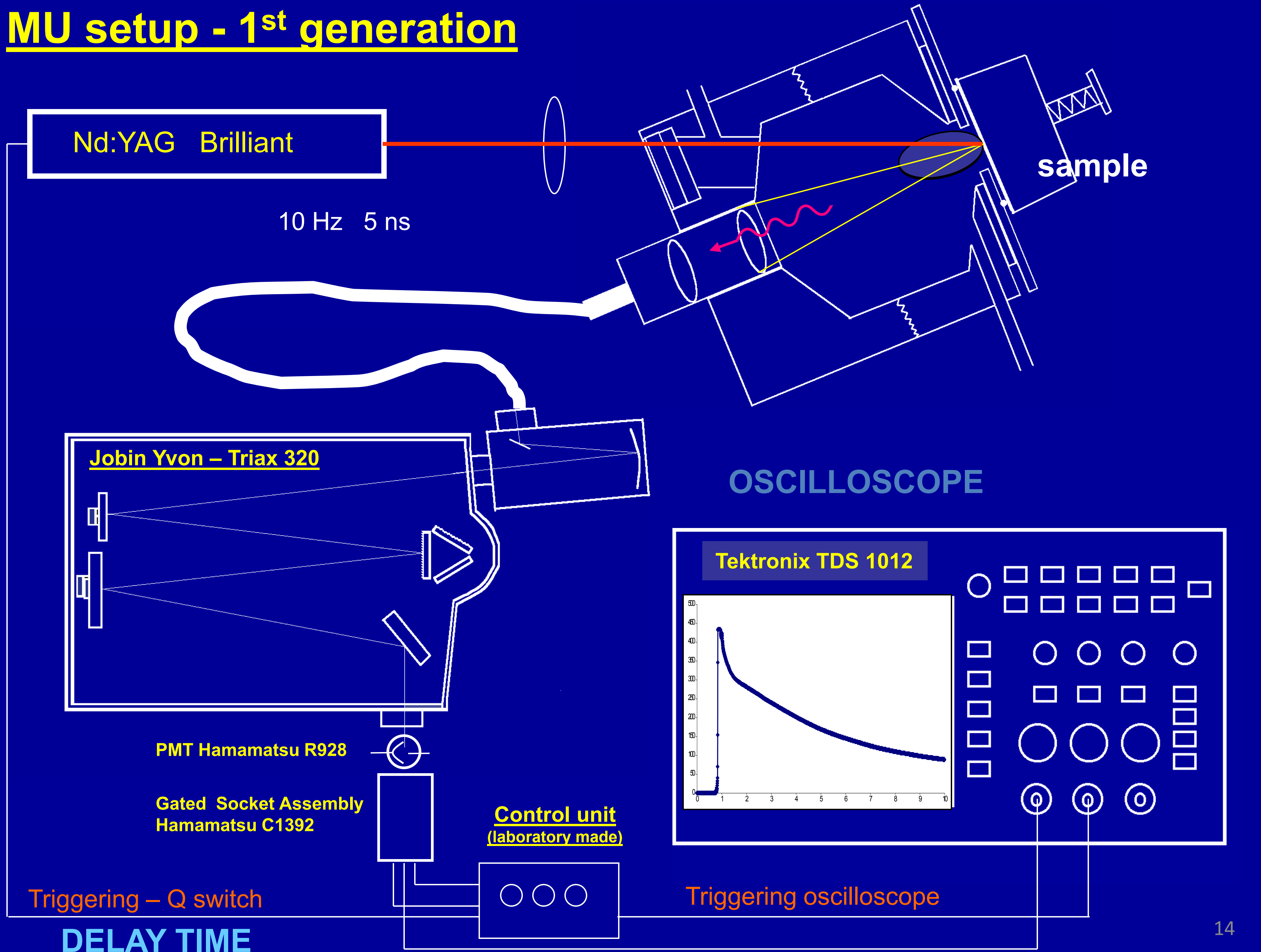

MU setup - 1st generation

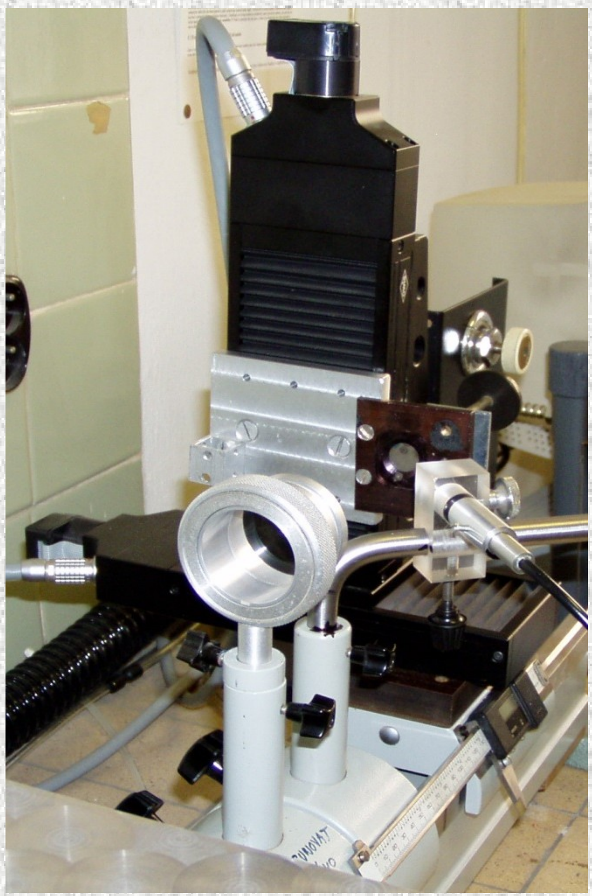

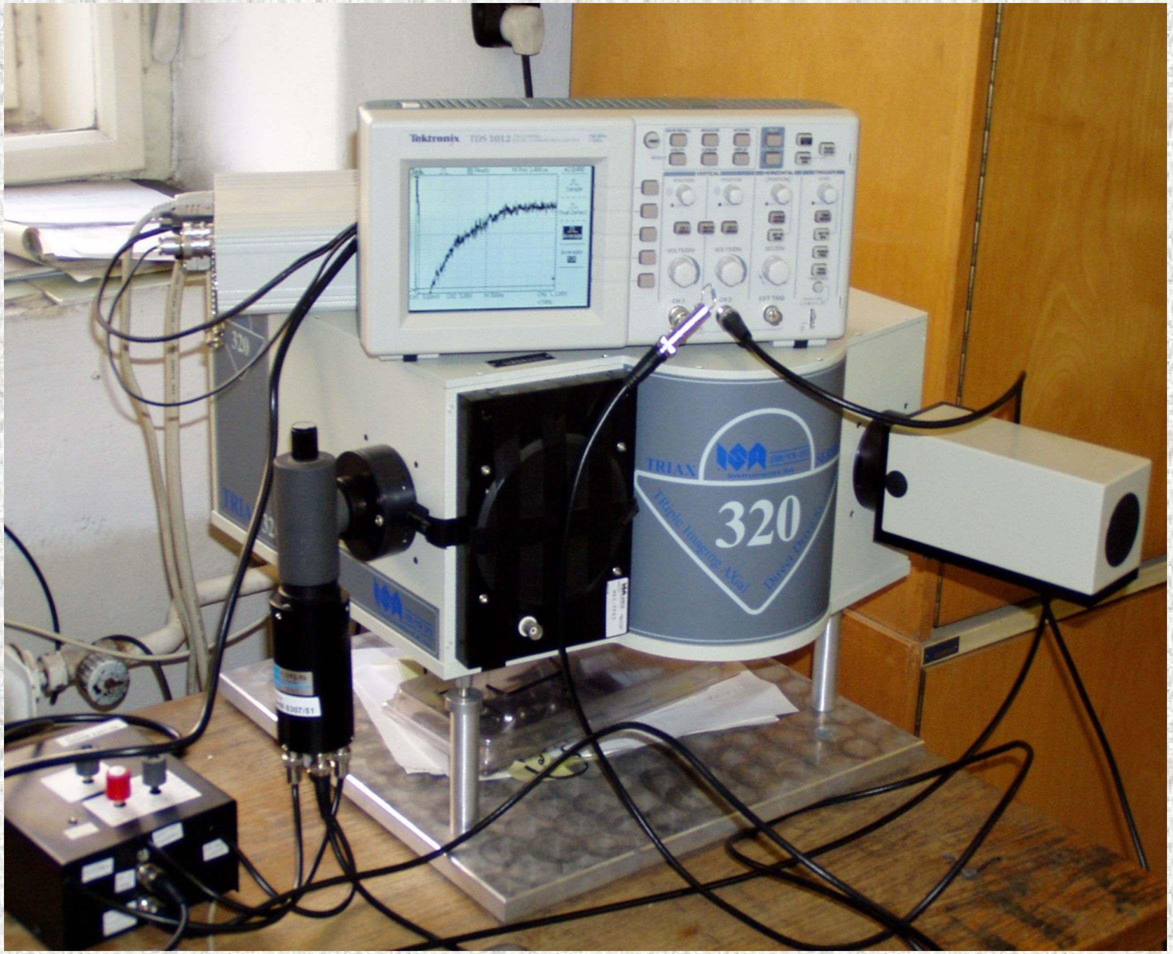

x,y stage   OWIS
Nd:YAG Brilliant (Quantel)
glass lens
optical fiber

Monochromator TRIAX 320 (Czerny – Turner 320 mm)
PMT Hamamatsu R928
Control of the PMT by Q – switch pulse
Oscilloscope TDS 1012

MU setup - 2nd generation

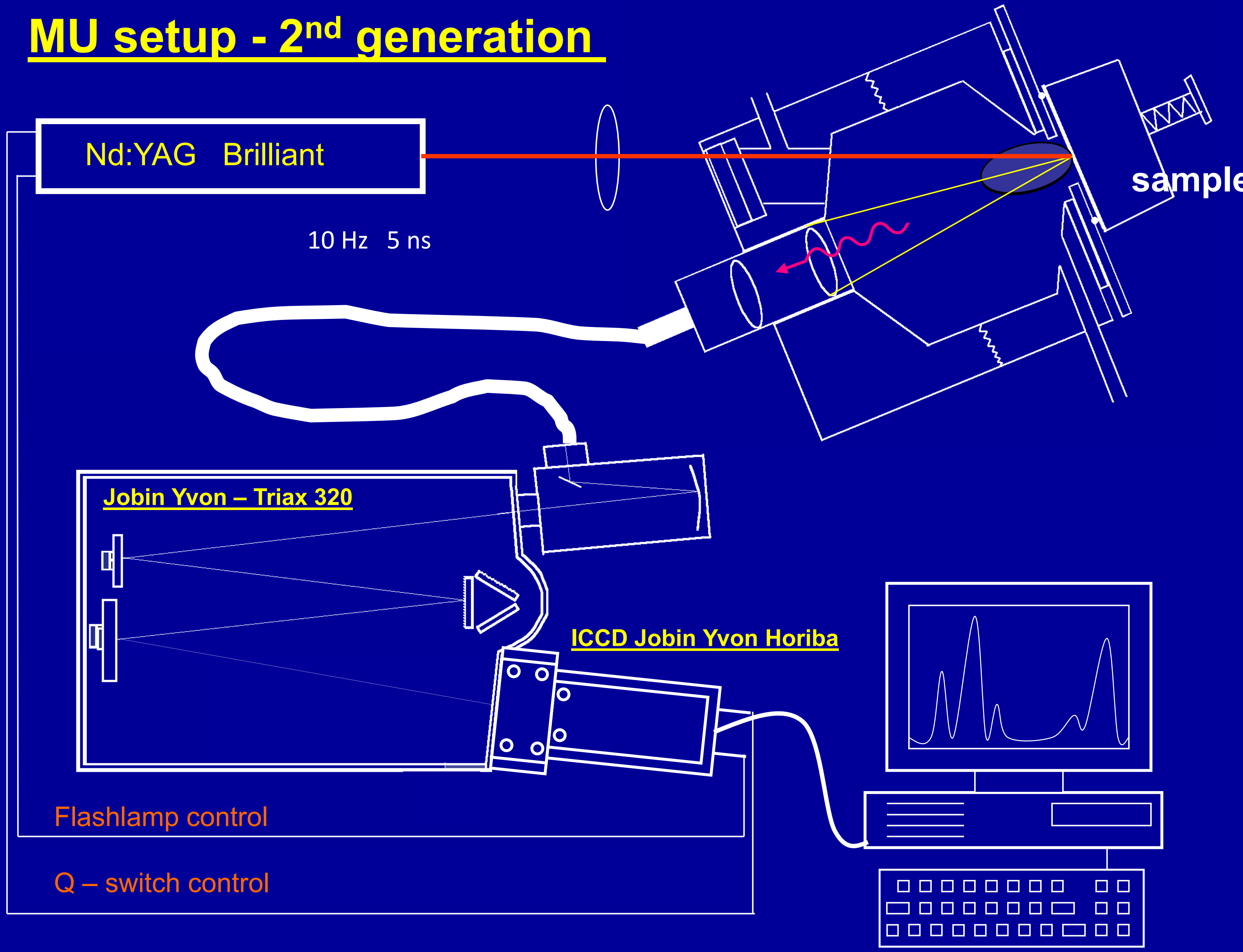

LA-ICP-OES

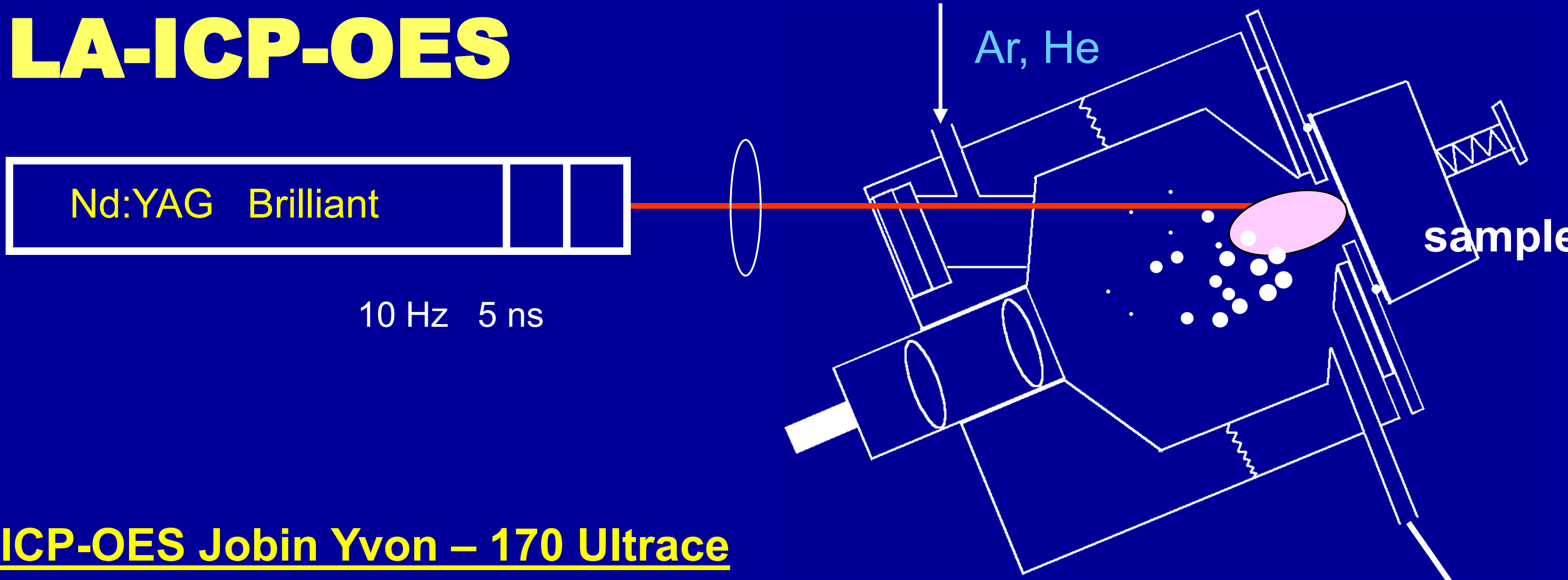

ICP-OES Jobin Yvon – 170 Ultrace

POLYCHROMATOR

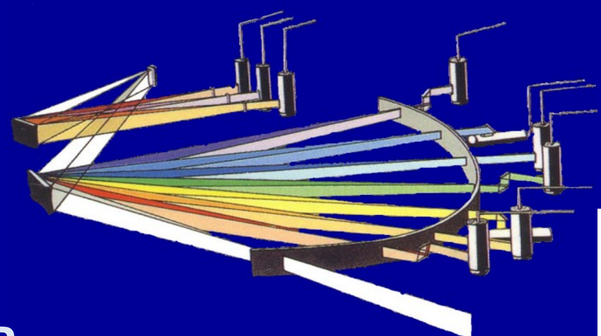

MONOCHROMATOR

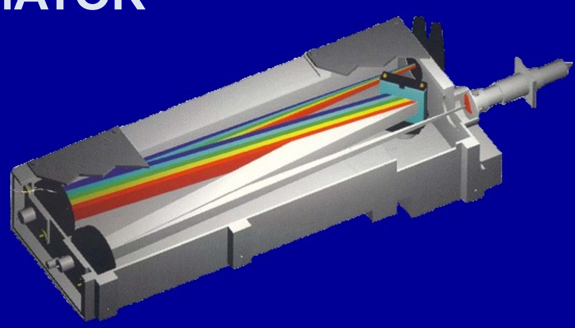

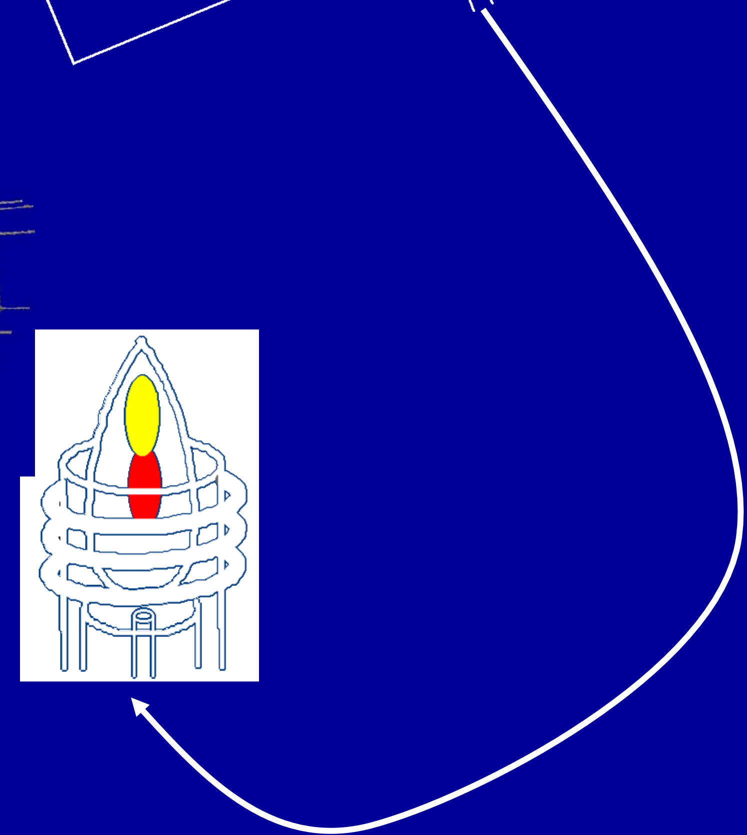

MU setup - 3rd generation

Double pulse technique (DP-LIBS)

Emission enhancement

- plasma volume increasing
- higher temperature
- longer decay time
- S/N enhancement

Decreasing of LOD up to two orders of magnitude

New Wave, UP 266 MACRO
Nd:YAG laser @ 266 nm (4-th harmonic frequency)
Second laser pulse Nd:YAG (Quantel Brilliant) @1064 nm

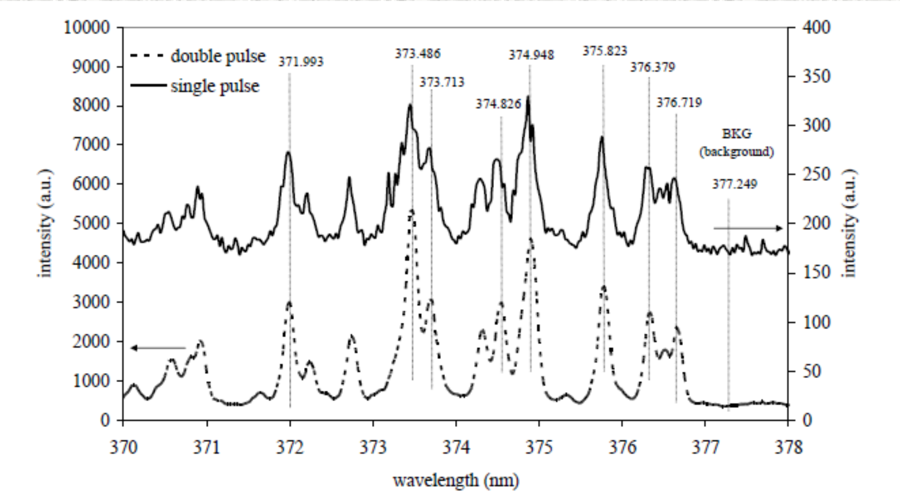

Comparison of the single and double-pulse signals in spectral region of selected iron lines

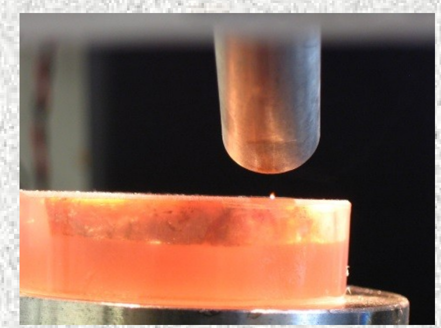

Single Pulse

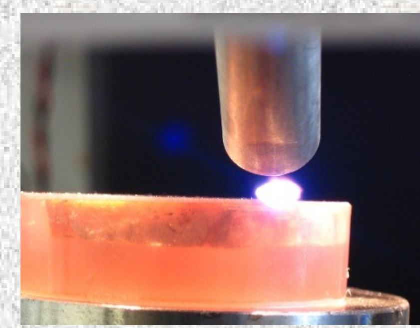

Double Pulse

Novotny, K.; Lutzky, F.; Galiova, M.; Kaiser, J.; Malina, R.; Kanicky, V.; Otruba, V., Double pulse laser ablation and plasma: time resolved spectral measurements. *Chemicke Listy* 2008, 102, S1399-S1402.

MU setup - 3rd generation

SIMULTANEOUS DP-LIBS AND LASER ABLATION ICP-OES SYSTEM

designed by utilizing a modified commercially available laser ablation system
(New Wave, UP 266 MACRO)

- no modification of the original optics - possible to use all advantages of the original arrangement
- spot ablation for depth profiling, line scanning for lateral analysis and raster scanning for bulk or surface analysis.
- second re-heating laser pulse (Quantel Brilliant) is delivered orthogonally
  (periscope arrangement allowing precise laser beam positioning)

- two digital delay generators DG 645
- collection optics for emission transport to the monochromator Triax 320 (Jobin-Yvon)
- ICCD Princeton Instruments PI MAX-3
- sample holders
  (different size and shape)

For LA-ICP-OES experiments the original ablation chamber was replaced with a special laboratory made chamber

- window for entering the second orthogonal laser pulse
- window for collection of LIP emission
- stage for sample height alignment

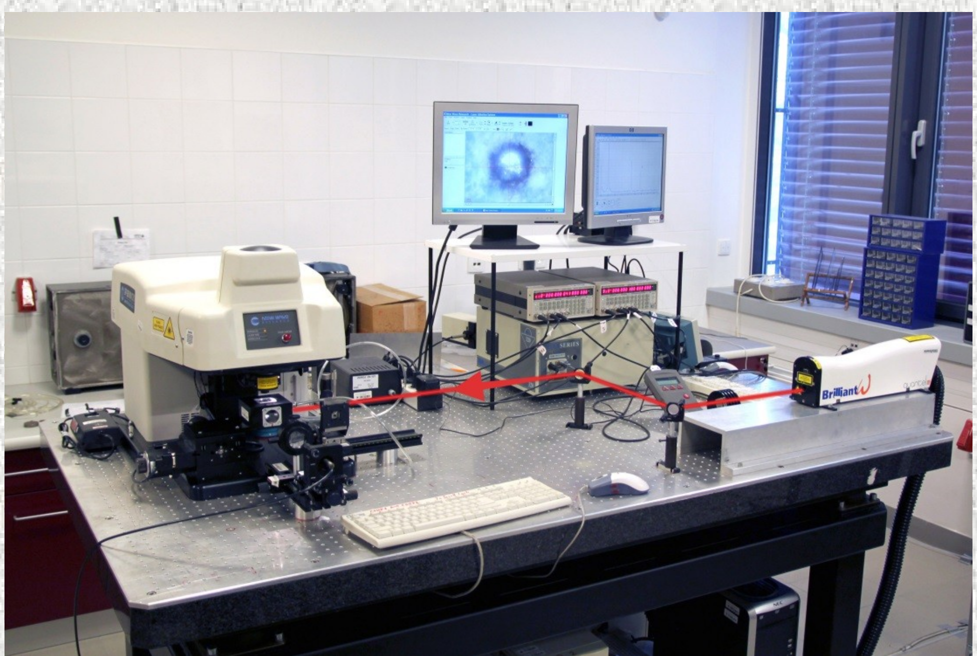

ALATION CHAMBER FOR SIMULTANEOUS DP-LIBS AND LA- ICP-OES/MS

Construction in cooperation with Institute of Physical Engineering BUT Brno (prof. J. Kaiser)

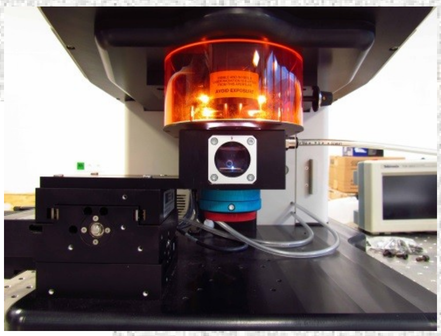

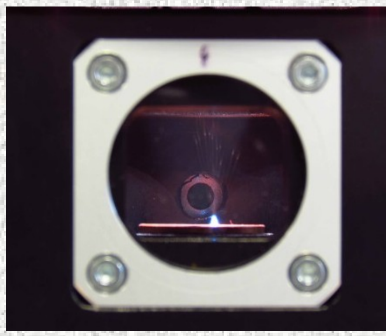

- compatible with the UP 266 Macro and UP-213 laser ablation systems
- ablation pulse led through the window from above
- re-heating pulse focused through the second window from the right side
- collection of LIP emission through third window at the front side
- oblique jets for carrier gas input
- aerosol output near the ablated sample surface
- vertically adjustable sample stage
- exchangeable inner rings to minimize the inner chamber volume

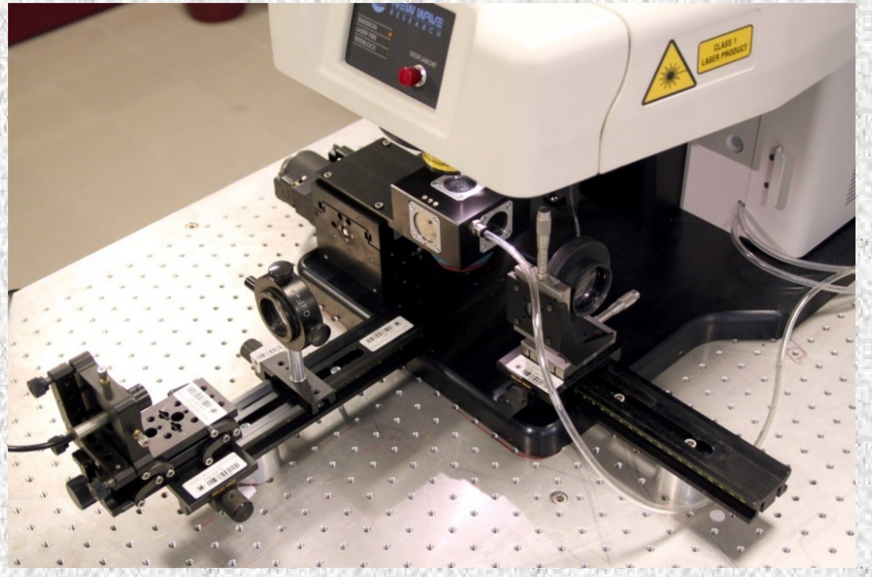

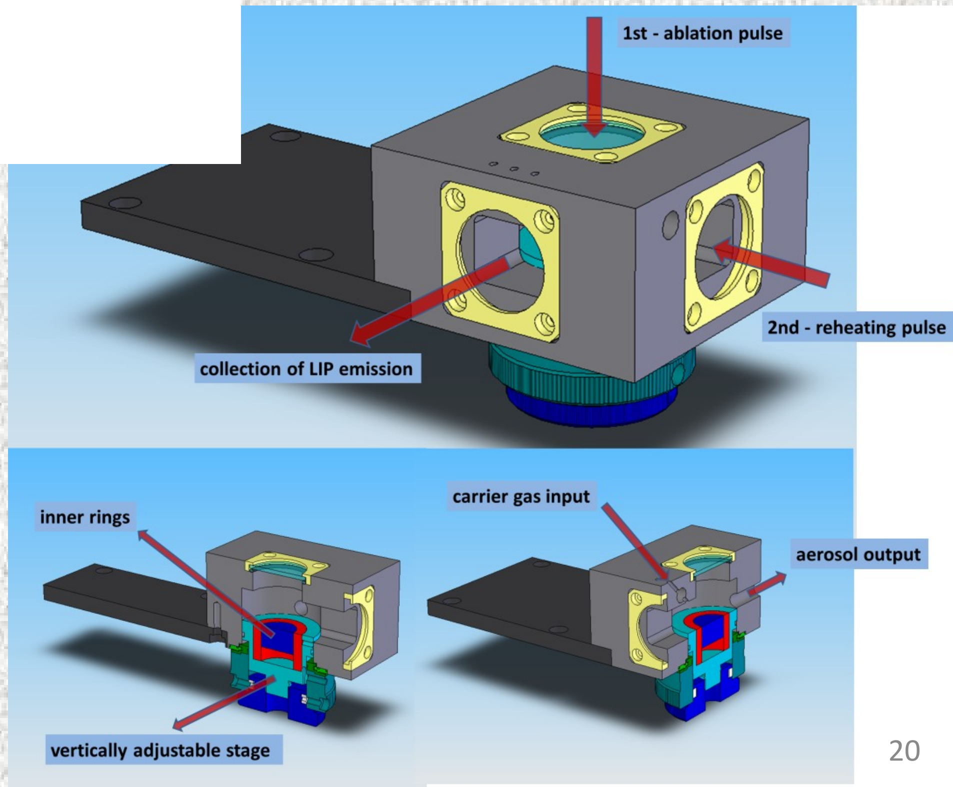

Instrumentation - Summary

1st generation

- Nd: YAG laser Brilliant (1064, 532 or 266 nm)
- monochromator Jobin Yvon TRIAX 320 (f=320 mm, three gratings – 1200, 2400 and 3600 g/mm)
- photomultiplier Hamamatsu gated by a laboratory-built control unit
- **time resolved emission signal at given wavelength**
- **laboratory-made aluminum ablation chamber - different ablation atmosphere**
  - connection to ICP OES

2nd generation

- **ICCD camera Jobin Yvon Horiba (iStar Andor)**

3rd generation

- **orthogonal double pulse configuration**
- laser ablation system New Wave UP 266 MACRO
- ablation chamber for **simultaneous DP-LIBS and double pulse LA-ICP-OES**
- sample surface monitoring by the internal CCD camera
- easy settings of all laser and detection parameters
- **programmable sample moving - depth profiling, line scanning or raster scanning for bulk or surface analysis**
- **single or double pulse experiments**
- detection by PMT or ICCD

Depth profiling

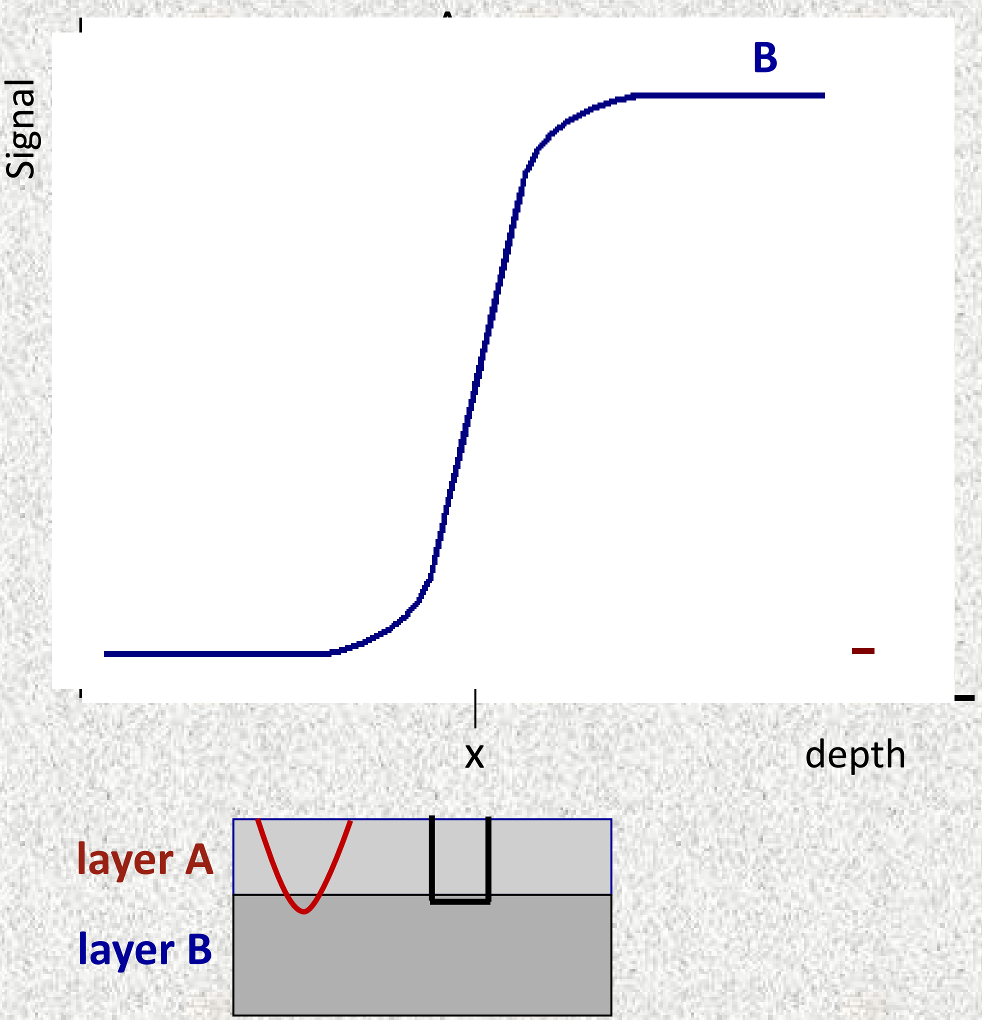

Depth profiling by LIBS

- from nanometer to millimeter scale
- no or minimal sample preparation
- without restrictions on the shape, size or conductivity
- under atmospheric conditions
- on-line and in situ measurement

Δz – depth resolution

defined by convention: depth range over which the signal changes from 84 to 16% of its full value

$$\Delta z = \Delta p \; AAR$$

Δp – number of laser shots needed to reach 84 and 16% of signal

AAR – averaged ablation rate

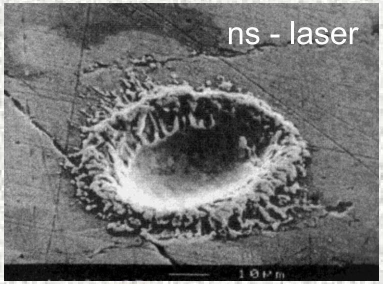

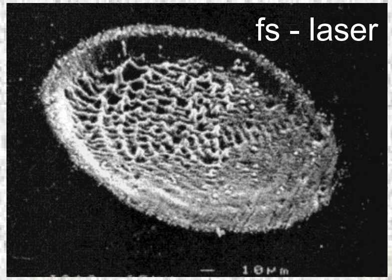

K. Niemax, Laser ablation – reflection on a very complex technique for solid sampling, *Fresenius J. Anal. Chem.* (2001) 370:332-340)

Depth profiling

(zinc-coated iron sheets)

Different manufactures and different zinc-coating thicknesses: previously analyzed by glow discharge optical emission spectrometry

Hoesch Stahl (20 µm)

electroplated Zn coating, Sollac (10 µm)

Aluzink, SSAB (24 µm)

Galfan, Voest Alpine (6 µm)

Galvanneal, British Steel (9 µm)

Optimized parameters

- laser pulse energy
- focusing condition
- different surrounding gases
- delay time

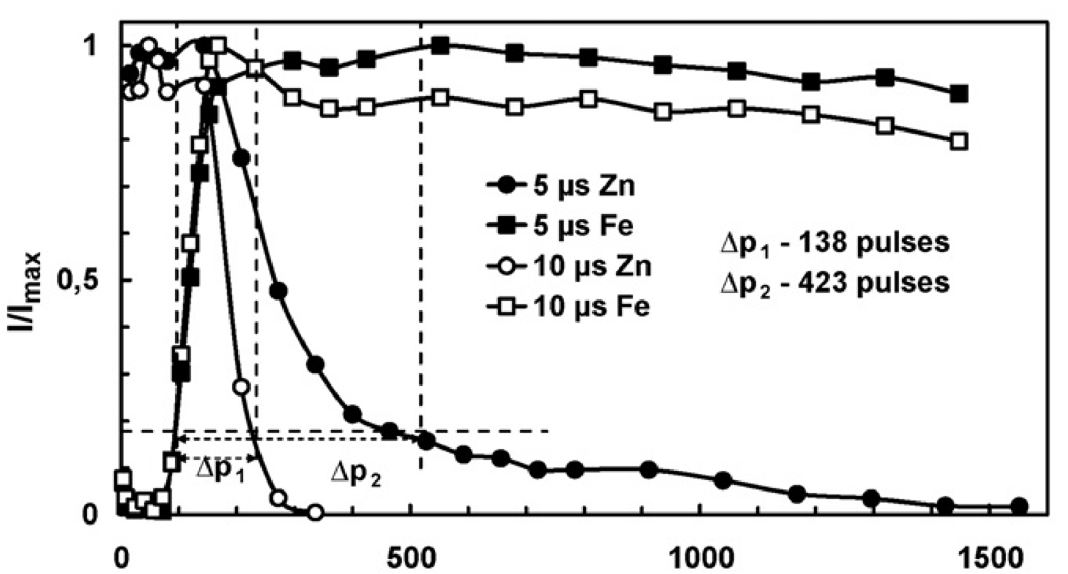

Depth profile of electroplated Zn in helium focusing at -20 mm. Comparison of LIBS signals of Zn(I) 280.08 nm and Fe(I) 344.06 nm at 5 and 10 ms delay times. Ablation was performed with an energy of 100 mJ/pulse.

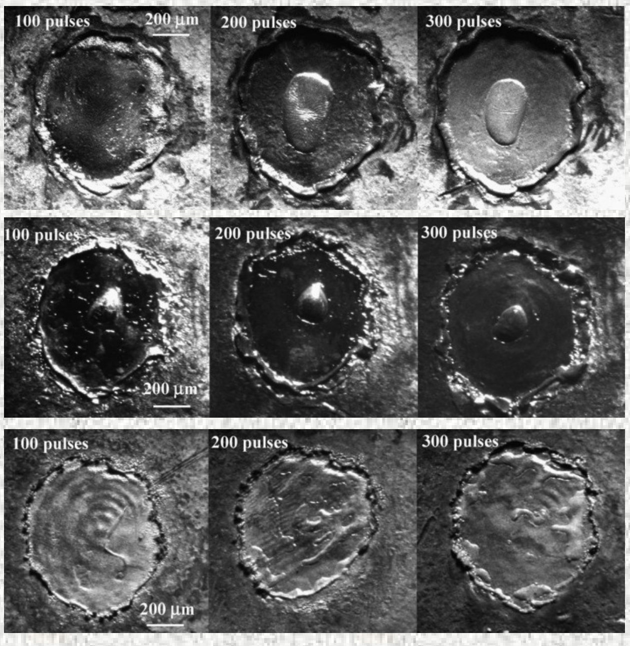

air

Ar

He

Novotny, K.; Vaculovic, T.; Galiova, M.; Otruba, V.; Kanicky, V.; Kaiser, J.; Liska, M.; Samek, O.; Malina, R.; Palenikova, K., The use of zinc and iron emission lines in the depth profile analysis of zinc-coated steel. *Applied Surface Science* 2007, 253, 3834-3842.

Depth profiling

(ceramic tiles)

Model sample of glazed silicate ceramics

- well-defined average contents of constituents
- reproducible production series

Oxide	Wt.%	
	Glaze	Ceramic body
SiO_2	56.84	66.11
Al_2O_3	7.75	18.99
Fe_2O_3	0.35	1.23
TiO_2	0.09	0.68
CaO	6.03	9.79
MgO	0.54	1.49
K_2O	2.51	1.42
Na_2O	0.20	0.29
ZrO_2	0.22	0.00
ZnO	9.26	0.00
BaO	1.96	0.00
SrO	0.10	0.00
PbO	7.37	0.00
CuO	0.06	0.00
Cr_2O_3	6.18	0.00

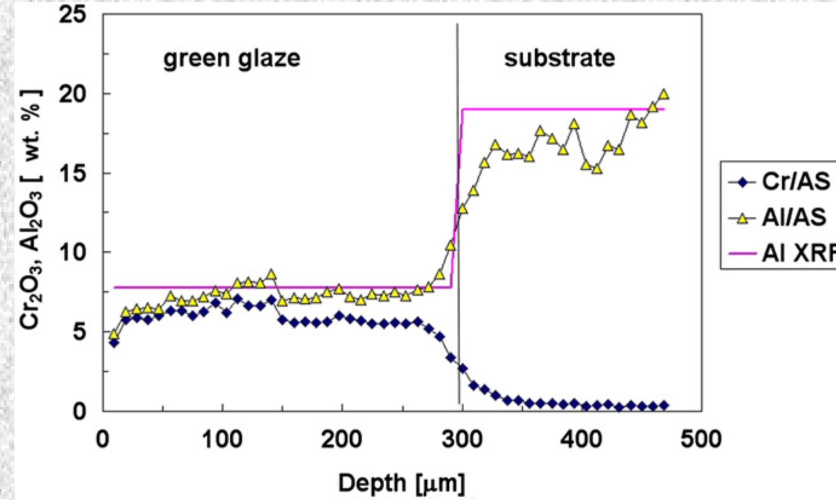

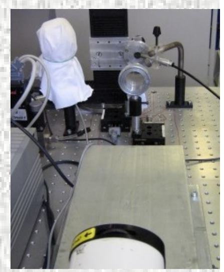

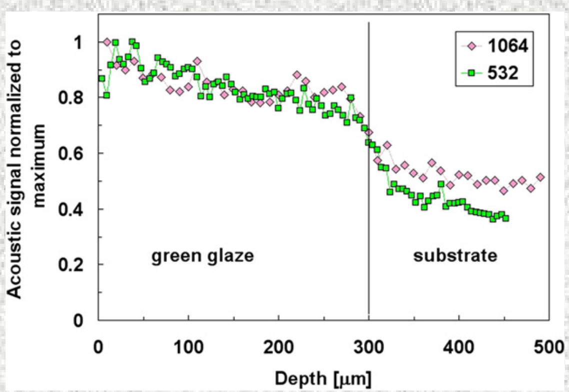

decrease in the optical emission during ablation was successfully compensated by normalization to the acoustic signal

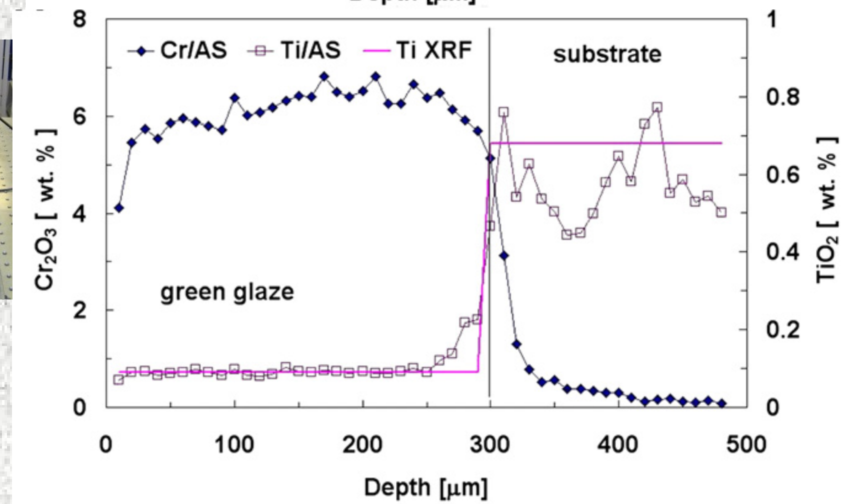

Depth profile of the green tile acquired for Al(I) 309.271 nm, Cr(I) 295.368 nm and Ti(II(334.904 nm.

Hrdlicka, A.; Zaoralkova, L.; Galiova, M.; Ctvrtnickova, T.; Kanicky, V.; Otruba, V.; Novotny, K.; Krasensky, P.; Kaiser, J.; Malina, R.; Palenikova, K., Correlation of acoustic and optical emission signals produced at 1064 and 532 nm laser-induced breakdown spectroscopy (LIBS) of glazed wall tiles. *Spectrochimica Acta Part B-Atomic Spectroscopy* 2009, 64, 74-78.

Mapping and depth profiling

(ceramic tiles)

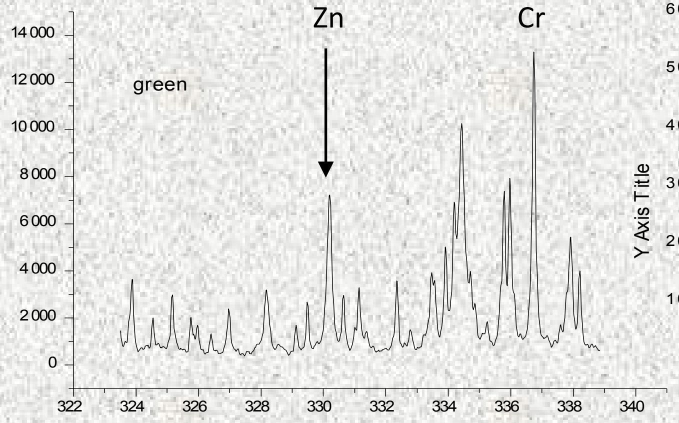

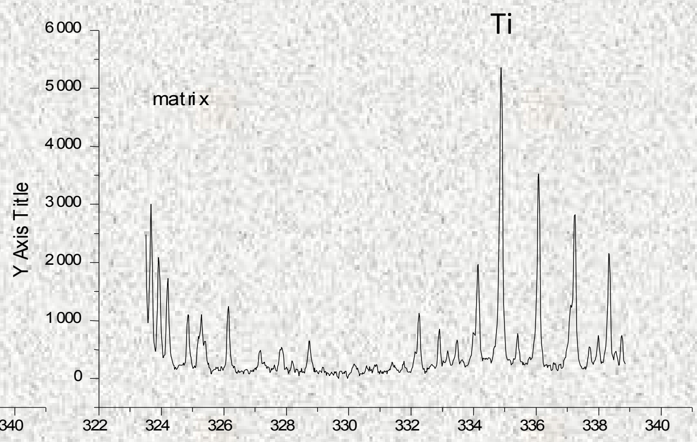

Ti(II) 334.9 nm
Cr(II) 336.8 nm
Zn(I) 330.29nm

ablation craters

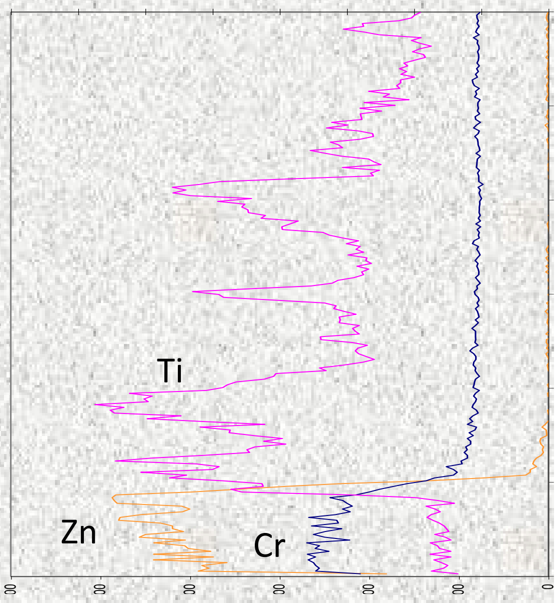

Normalized intensity

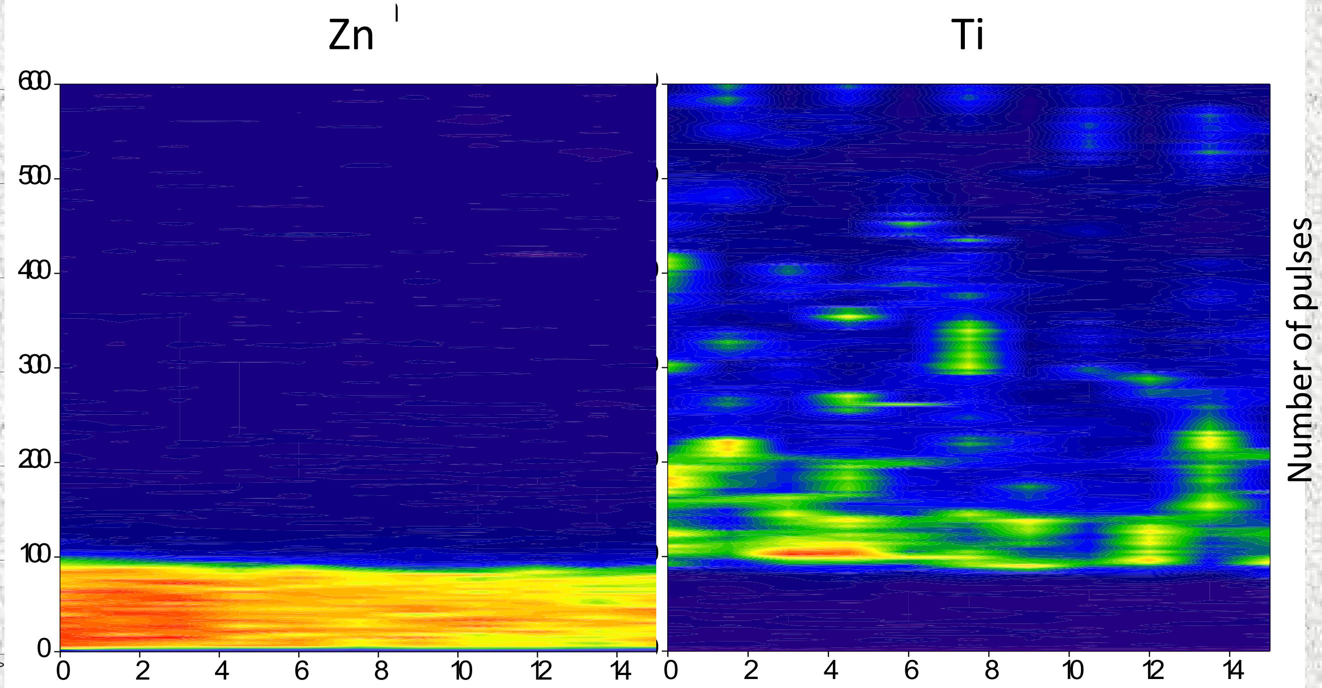

Position on the sample

Position on the sample

Mapping of elemental distribution

(plant samples)

Cleaning of metal contaminated soil - **PHYTOREMEDIATION**

resistant, strong tolerance, effective plant-transport mechanisms, high accumulation, high biomass, fast growth

herbs: *Zea mays, Helianthus annuus ...*

trees: *Betula pendula, Populus tremula ...*

	Sample		Investigated part	Monitored element	Method		
					LIBS		LA-ICP-MS
					SP	DP	
Cultivated plants	*Helianthus annuus*		leaves, stems, roots	Pb, Cd, Mg, K, Ag, Cu	X		X
	Zea mays		leaves, stems, roots	Pb, Mg, Fe	X		X
	Cornus stolonifera		leaves	Fe	X		
	Lactuca sativa L.		leaves	Pb, Mg	X		
	Picea abies	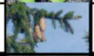	needles, twigs	Cu, Ca		X	
Natural plants	*Pinus sylvestris*		needles	Cu, Ca	X		
	Populus tremula		leaves	Cu, Ca	X		
	Betula pendula		leaves	Cu, Ca	X		
	Picea abies		needles, twigs	Cu, Ca	X		

Samples from naturally growing trees

recultivated sludge bed in locality **Smolník (Slovakia)**

Laboratory cultivated plants

Department of Chemistry and Biochemistry, Mendel University in Brno

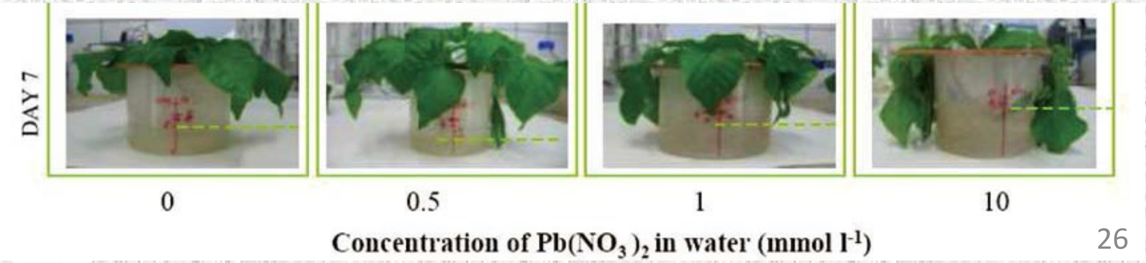

Mapping of elemental distribution

(plant samples)

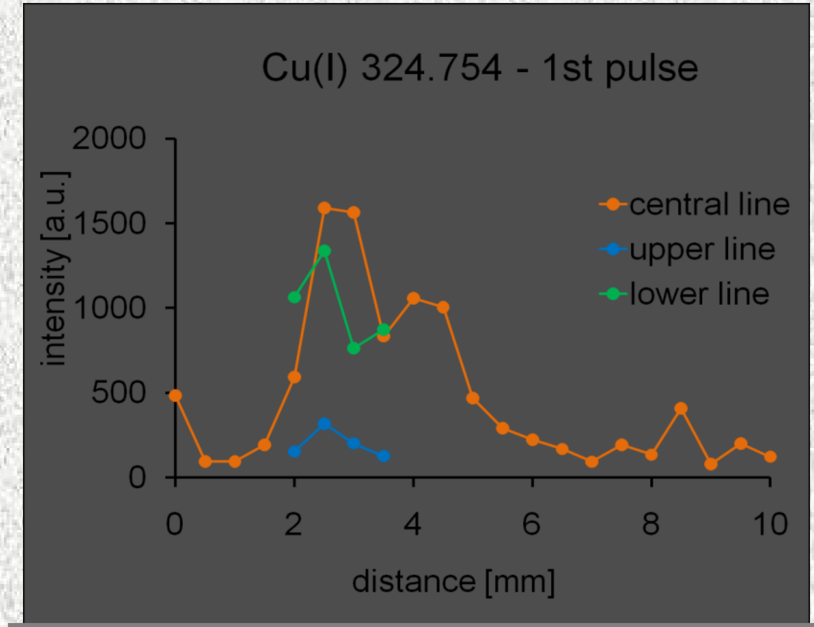

Smolník

Copper distribution in the needle of pine tree (***Pinus sylvestris***) obtained by LIBS **single pulse.**

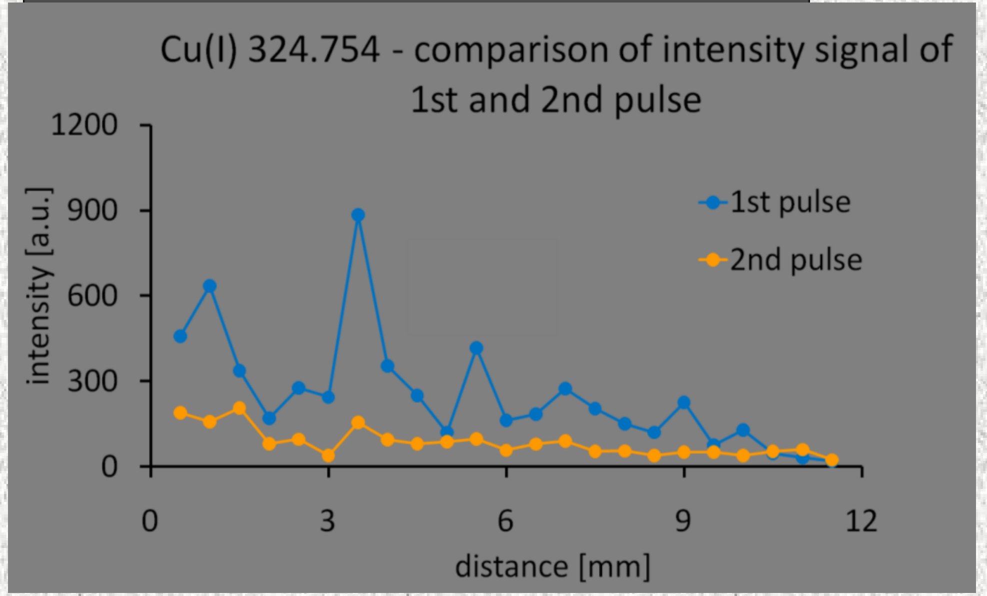

Copper distribution in central vein of the aspen leaf (***Populus tremula***) obtained by LIBS **single pulse**; two laser pulses on each point.

Mapping of elemental distribution

(plant samples)

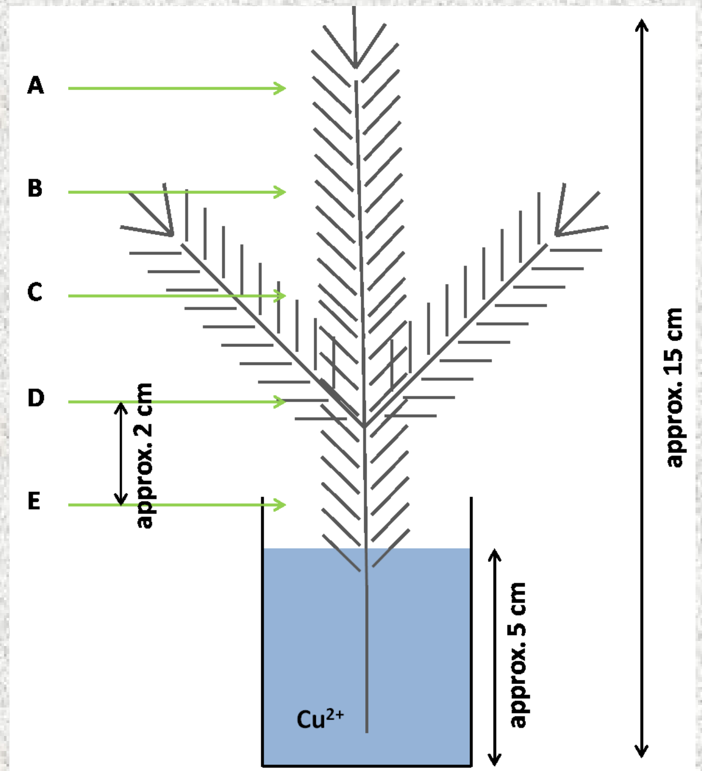

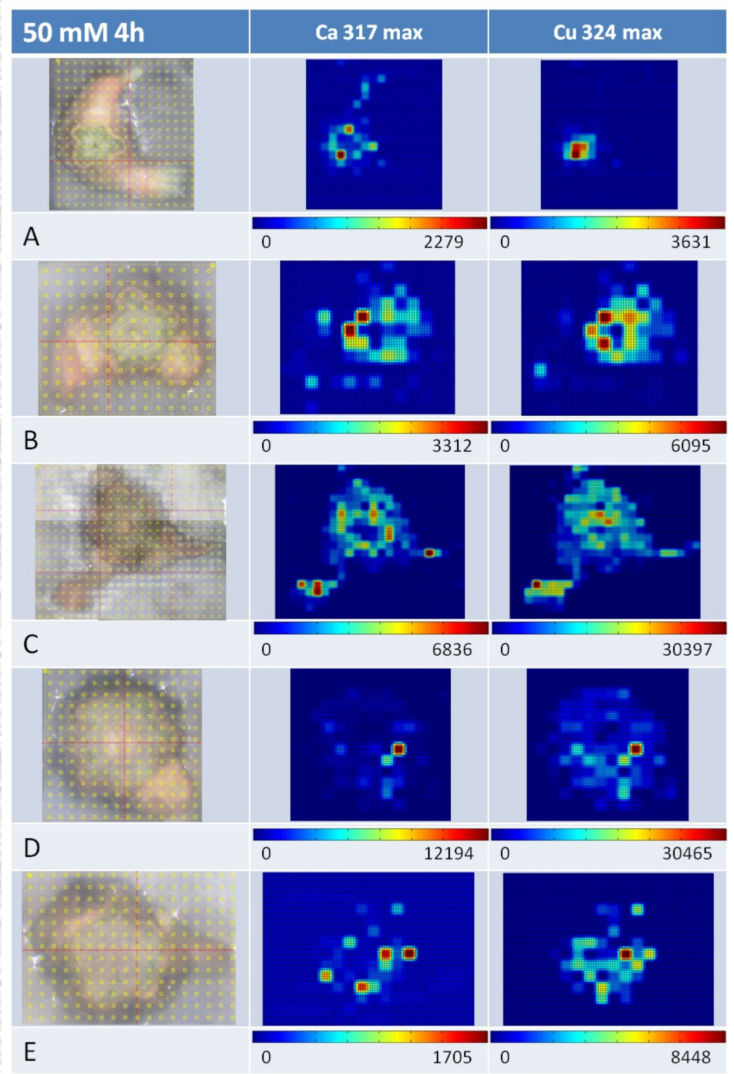

Example of copper and calcium distribution maps on cross sections of spruce twigs (*Picea abies*) **cultivated** in 50 mmol.l^{-1} $CuCl_2$ obtained by **LIBS double pulse**.

Point distance = 150 µm

Krajcarova, L.; Novotny, K.; Babula, P.; Provaznik, I.; Kucerova, P.; Adam, V.; Martin, M.Z.; Kizek, R.; Kaiser, J., Copper Transport and Accumulation in Spruce Stems (*Picea abies* (L.) Karsten) Revealed by Laser-Induced Breakdown Spectroscopy. *International Journal of Electrochemical Science,*2013, 8, 4485-4504.

Mapping of elemental distribution

(plant samples)

Mapping of accumulation and distribution of heavy metal (lead) and nutrition elements (potassium) in leaves of *Capsicum annuum L*. samples.

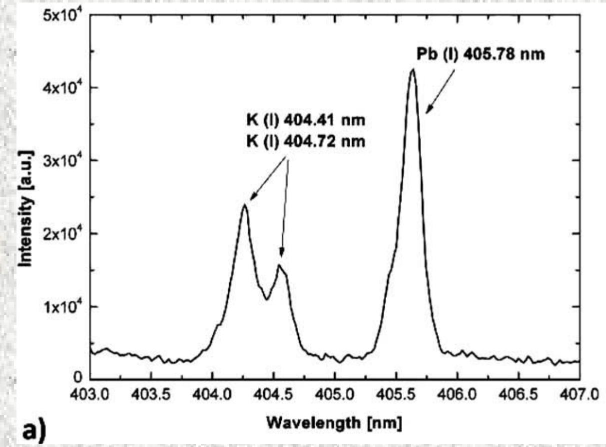

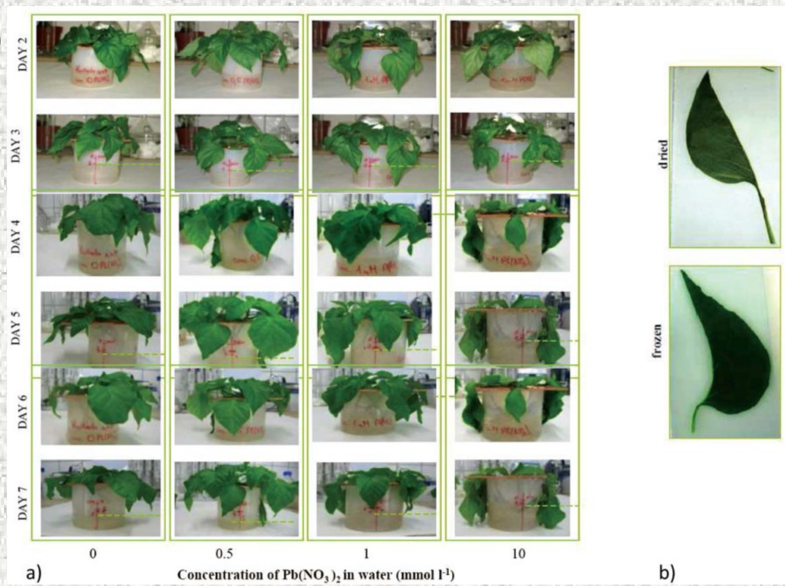

(a) Set of *C. annuum L.* samples used for monitoring of effects of lead(II) ions. (b) Example of the investigated *C. annuum* L. leaves.

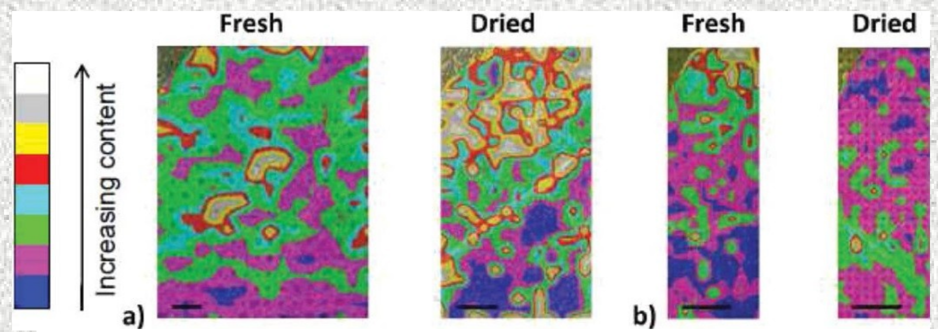

The maps of K obtained from the studied area of the 2 days 10 mmol L^{-1} $Pb(NO_3)_2$ treated *C. annuum L.* leaf. The K distribution in fresh (frozen) and dried samples measured by (a) LIBS and (b) LA-ICP-MS.

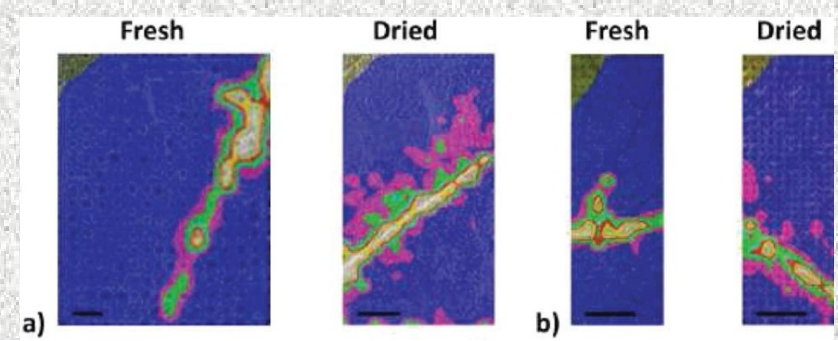

The maps of Pb obtained from the studied area of the 2 days 10 mmol L^{-1} $Pb(NO_3)_2$ treated *C. annuum L.* leaf. The K distribution in fresh (frozen) and dried leaf measured by (a) LIBS and (b) LA-ICP-MS.

Galiova, M.; Kaiser, J.; Novotny, K.; Hartl, M.; Kizek, R.; Babula, P., Utilization of Laser-Assisted Analytical Methods for Monitoring of Lead and Nutrition Elements Distribution in Fresh and Dried Capsicum annuum L. Leaves. *Microscopy Research and Technique* 2011, 74, 845-852.

Elemental mapping

(geological sample)

Comparison study:

multi-element (Ca, Al, Fe, Mn) mappings of a granite sample surface performed by **LIBS** and subsequently by **LA-ICP-MS** analysis

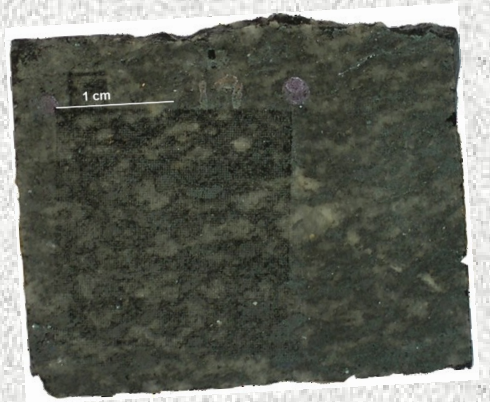

The 2 x 2 cm^2 area of the granite was sampled with a spatial resolution of 200 μm (the distance of the LIBS and LA-ICP-MS craters).

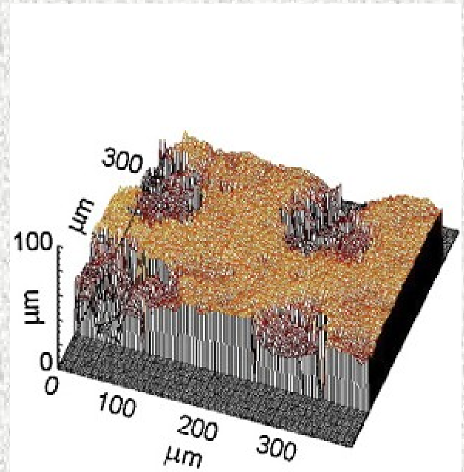

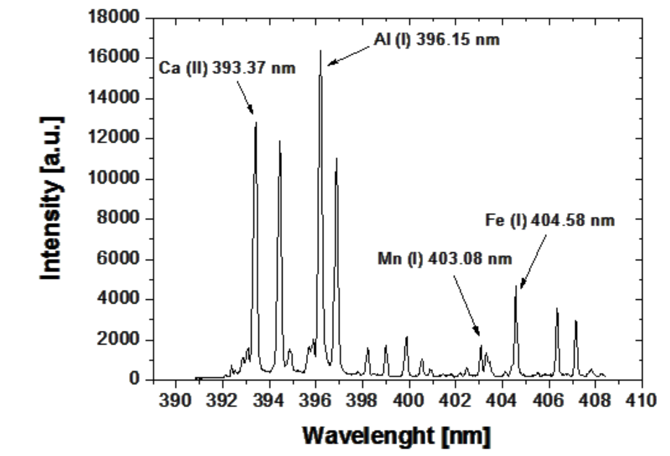

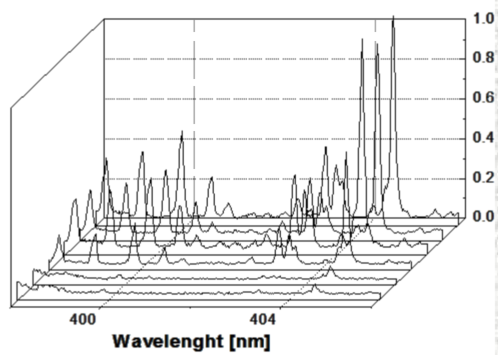

Set of normalised spectrums obtained by six subsequent pulses from the different places of the sample.

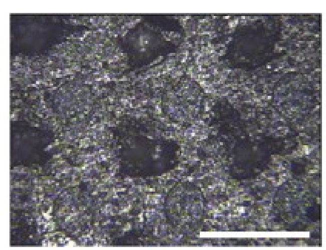

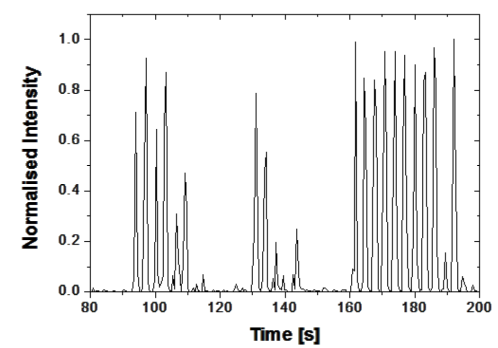

Typical LA-ICP-MS signal for Fe monitoring obtained for ~40 ablation craters.

Novotny, K.; Kaiser, J.; Galiova, M.; Konecna, V.; Novotny, J.; Malina, R.; Liska, M.; Kanicky, V.; Otruba, V., Mapping of different structures on large area of granite sample using laser-ablation based analytical techniques, an exploratory study. *Spectrochimica Acta Part B-Atomic Spectroscopy* 2008, 63, 1139-1144.

Elemental mapping

(geological sample)

100×100 individual sample points to map an area of 20×20 mm^2

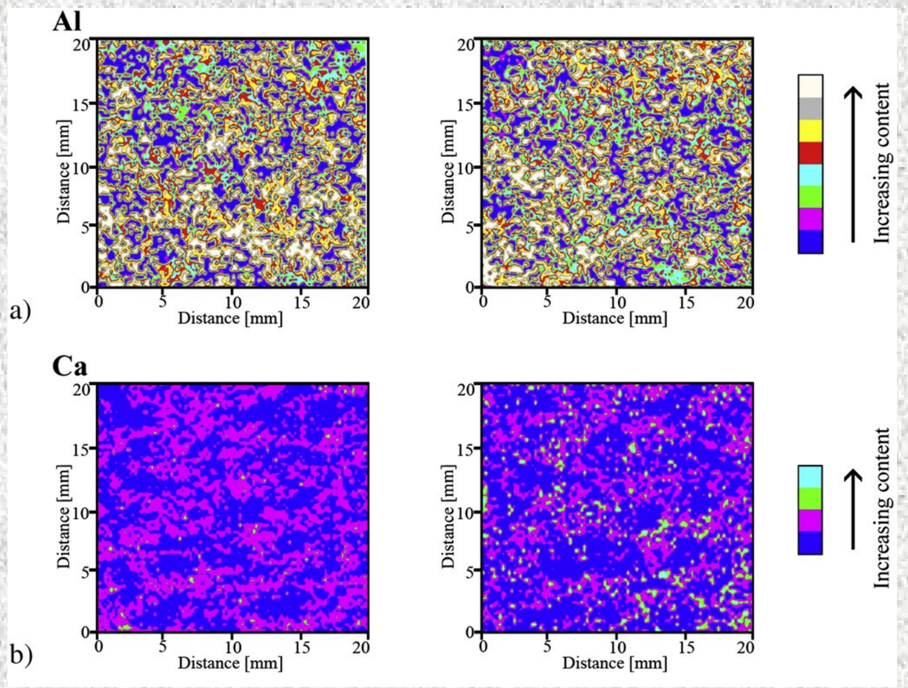

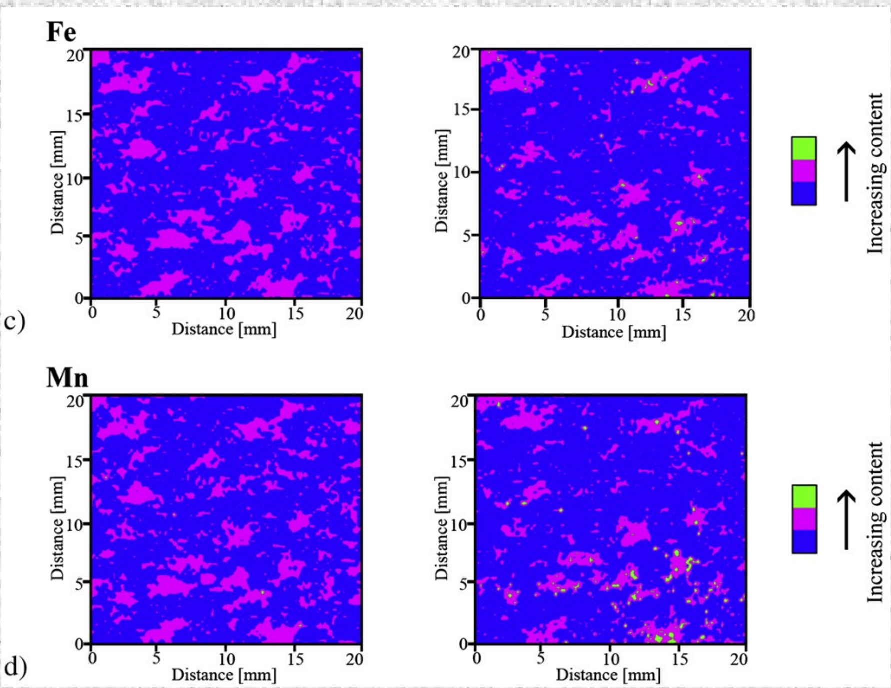

LIBS LA-ICP-MS LIBS LA-ICP-MS

Novotny, K.; Kaiser, J.; Galiova, M.; Konecna, V.; Novotny, J.; Malina, R.; Liska, M.; Kanicky, V.; Otruba, V., Mapping of different structures on large area of granite sample using laser-ablation based analytical techniques, an exploratory study. *Spectrochimica Acta Part B-Atomic Spectroscopy* 2008, 63, 1139-1144.

Elemental mapping

(teeth)

Upper palaeolithic reindeer tooth
locality at Moravany-Lopata, Western Slovakia

Fossil brown bear (*Ursus arctos*) was excavated at Dolní Věstonice II-Western Slope, South Moravia, Czech Republic.

Protemnodon - an extinct species of a kangaroo that lived about 50 000 years ago, found in Australian swamps

Elemental mapping

(teeth)

The estimation of the sample hardness via magnesium ionic to atomic line intensity. The estimated hardness characteristic was proved by microhardness measurements.

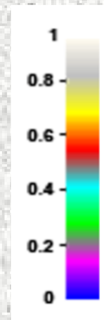

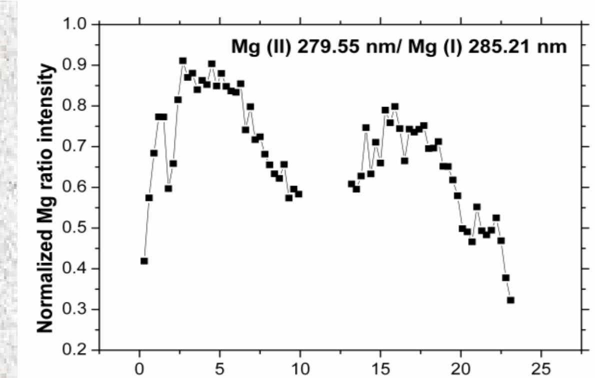

ETHOLOGY OF THE STUDIED FOSSIL BROWN BEAR

The seasonal fluctuations of the Sr/Ca and Sr/Ba detected by DP LIBS evidenced the migration of this bear between his hibernaculum's location and the place where the fossils were found.

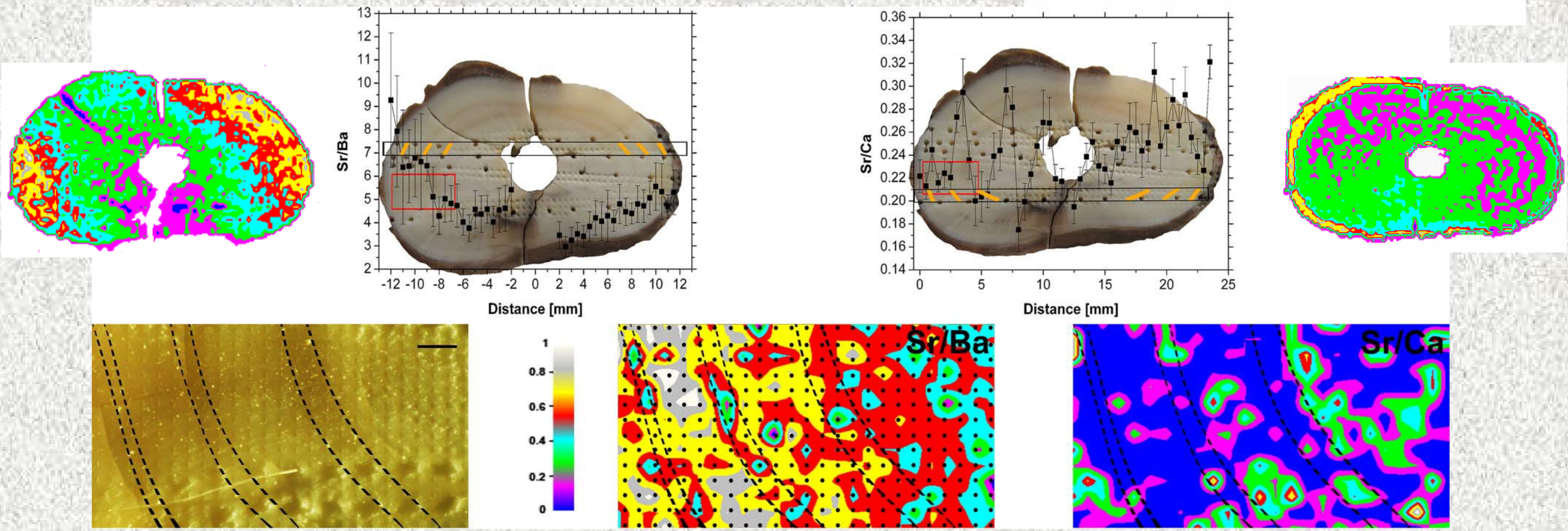

Sr/Ca and Sr/Ba ratios derived from LIBS line scan and LA-ICP-MS mapping; dotted lines represent the different regions (white, summer bands; brown, winter bands) of the tooth cross section. The bar has a length of 500 μm.

Galiova, M.; Kaiser, J.; Fortes, F. J.; Novotny, K.; Malina, R.; Prokes, L.; Hrdlicka, A.; Vaculovic, T.; Fisakova, M. N.; Svoboda, J.; Kanicky, V.; Laserna, J. J., Multielemental analysis of prehistoric animal teeth by laser-induced breakdown spectroscopy and laser ablation inductively coupled plasma mass spectrometry. *Applied Optics* 2010, 49, C191-C199.

Elemental mapping

(fossil snake vertebrae)

Elemental mapping of pathological bony tissue (*osteitis deformans* phases in fossil vertebrae)

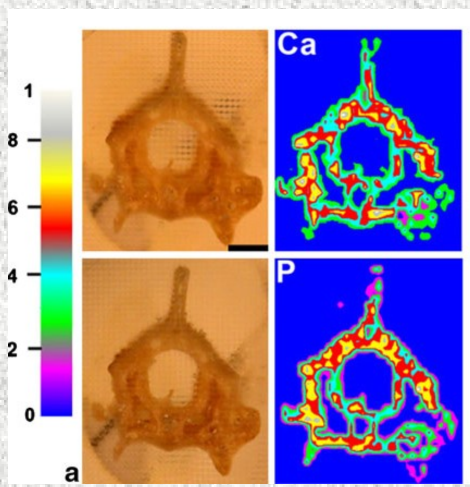

The fossil material:

Natrix natrix
Mladeč Caves excavation II
(Czech Republic),
Early Pleistocene

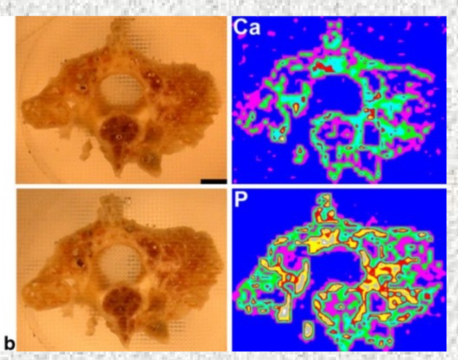

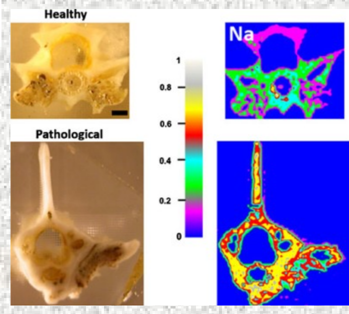

Lower Ca/P ratio indicating the later stage of the *osteitis deformans*.
Na content can be caused by metabolic derangement ("acidosis").

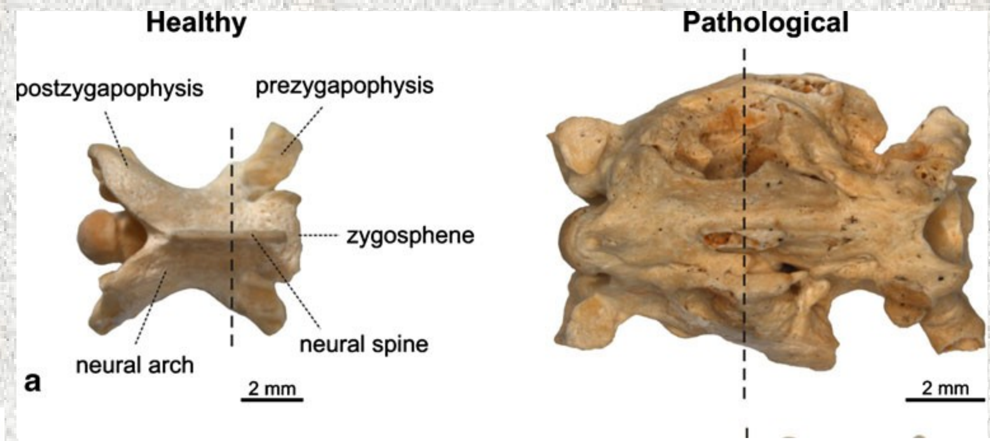

The photographs of the studied a fossil (*N. natrix*) snake vertebrae. The investigated healthy (the left images) and pathological (the right images) bones are shown.

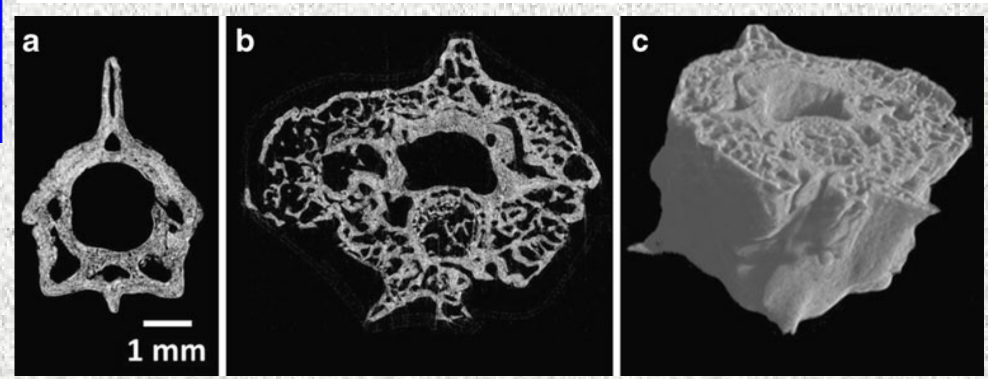

SR-µCT slices of **a** healthy and **b** pathological fossil snake vertebra together with c the 3D rendering of the investigated fossil snake vertebra segment

Galiova, M.; Kaiser, J.; Novotny, K.; Ivanov, M.; Fisakova, M. N.; Mancini, L.; Tromba, G.; Vaculovic, T.; Liska, M.; Kanicky, V., Investigation of the osteitis deformans phases in snake vertebrae by double-pulse laser-induced breakdown spectroscopy. *Analytical and Bioanalytical Chemistry* 2010, 398, 1095-1107.

Elemental mapping

(urinary stones)

Mineralized tissues and bio-mineral structures are “archives” related to living habits, nutrition and exposure to changing environmental conditions.

Line scans of the urinary concrement cross-sections may provide information about the accumulation history of the elements of interest.

Four categories of urinary stones: a) oxalates b) phosphates c) uric acid and d) cystine.

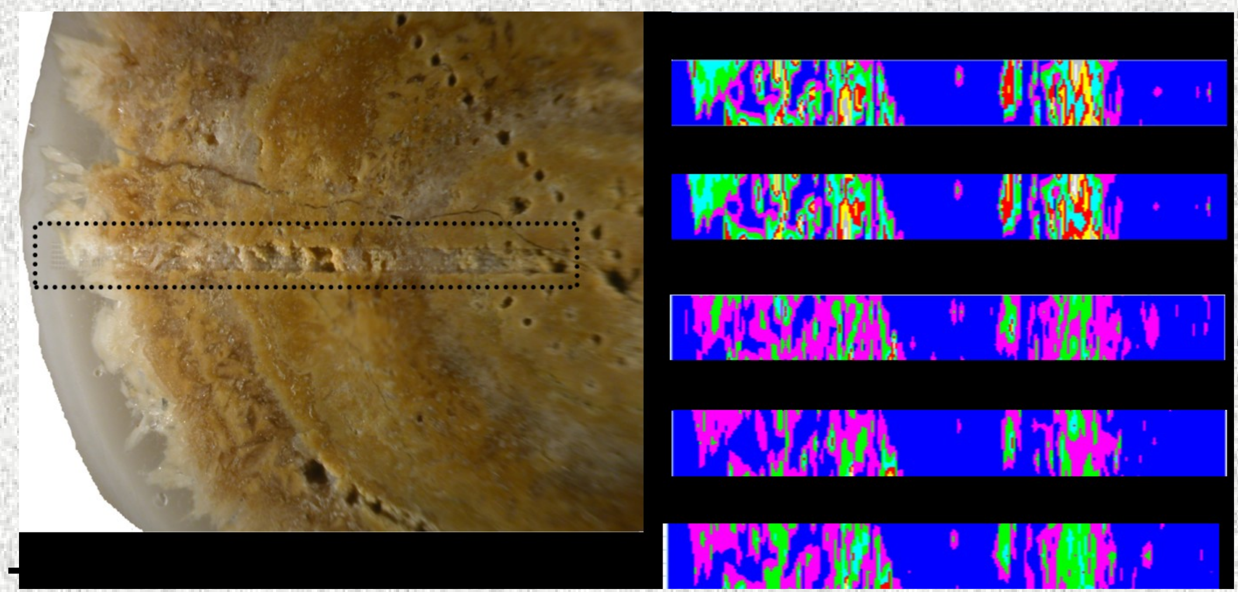

Correlation between calcium and phosphorus indicates the presence of apatite.

Distribution of iron is connected with accumulation of blood clot during the growth of urinary stones in the urinary bladder.

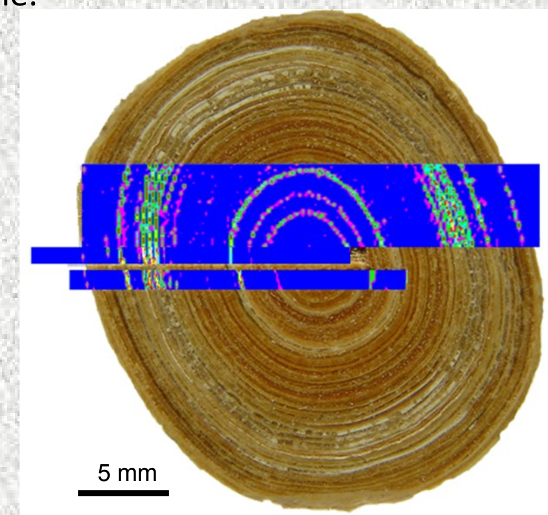

Ca distribution

Sample no. 10806: oval, ellipsoidal, pale yellow-brown zone.
The main components:
uric acid (90%)
weddellite $CaC_2O_4 \cdot 2\ H_2O$ (10%)

Powder samples

powdered tungsten carbide hard-metal precursors (WC/Co)

Samples: Pramet Tools, Šumperk, Czech Republic

The elemental composition of powders samples:

element	content % (m/m)
W	57–88
C	4.8–7.5
Co	3–10
Ti	0.04–9.6
Ta	0.1–8.2
Nb	0.05–3.4

preparation of pressed pellets with or without binder (binder powdered silver)

Element	Wavelength (nm)
Nb	405,89
Ta	648,53
Co	350,25
Ti	361,03

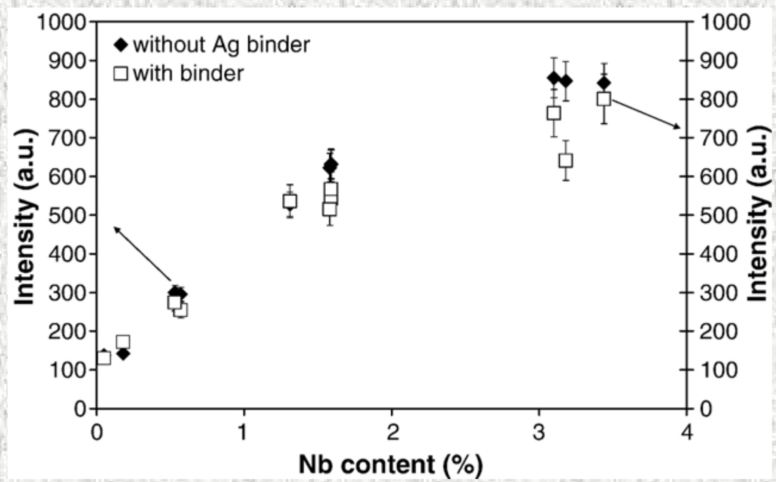

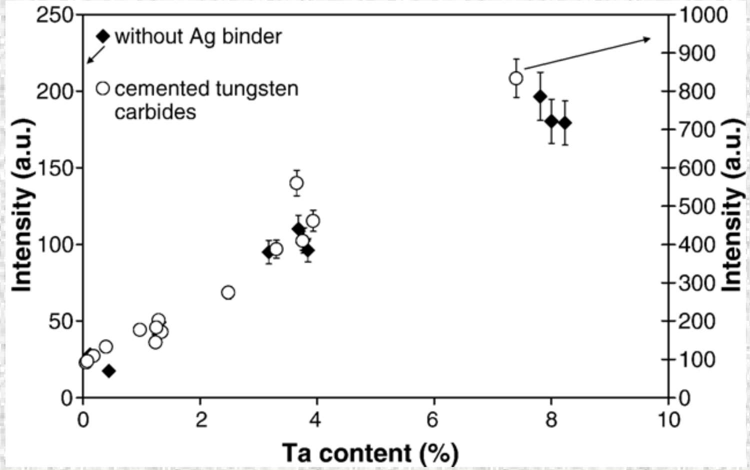

Novotny, K.; Stankova, A.; Haekkaenen, H.; Korppi-Tommola, J.; Otruba, V.; Kanicky, V., Analysis of powdered tungsten carbide hard-metal precursors and cemented compact tungsten carbides using laser-induced breakdown spectroscopy. *Spectrochimica Acta Part B-Atomic Spectroscopy* 2007, 62, 1567-1574.

Powder samples

calibration pellets (urinary stones)

Mineralogical composition of calibration pellets

Mineral / No. Sample	Apatite [%]	Struvite [%]	Uric acid [%]	Calcium oxalate [%]
8393	51.4	51.6	0	0
5056	60.0	40.0	0	0
5255	61.3	38.7	0	0
6686	56.5	43.5	0	0
6489	52.8	47.2	0	0
5397	6.1	93.9	0	0
5996	35.2	64.8	0	0
9130	61.4	38.6	0	0
6671	75.2	24,8	0	0
8365	13.4	1.2	0	85.4
6275	7.8	0.4	0	91.8
9081	1.1	0.2	0	98.7
5166	10.7	0.6	0	88.7
8500	0.1	0.1	42.2	57.6
7851	1.6	0.3	0	98.1
7301	0.1	0	36.5	63.4
6432	0.2	0	50.1	49.7
6585	0	0	52.6	47.4

Laser ablation LIBS (LA-LIBS)

(analytical LIBS plasma is completely separated from LA)

Comparison of LIBS and LA LIBS

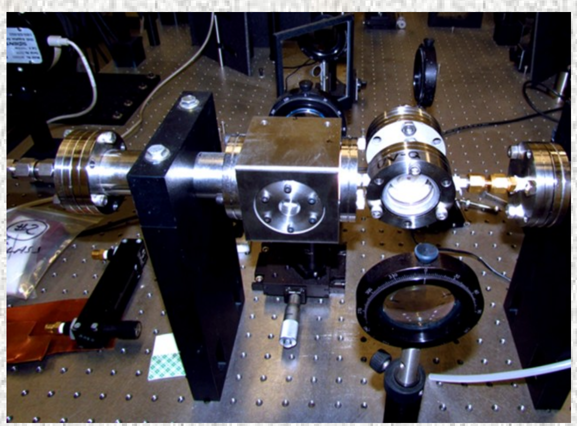

Problems with elements present in high content are related mainly to the LIBS technique and most probably they are connected to the processes in the LIP and self-absorption.

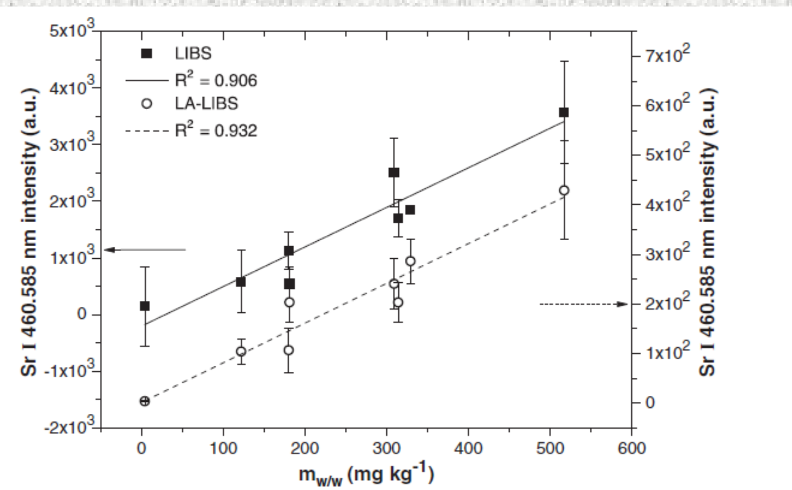

Comparison of LIBS and LA-LIBS calibration curves for Sr in phosphate matrix pellets.

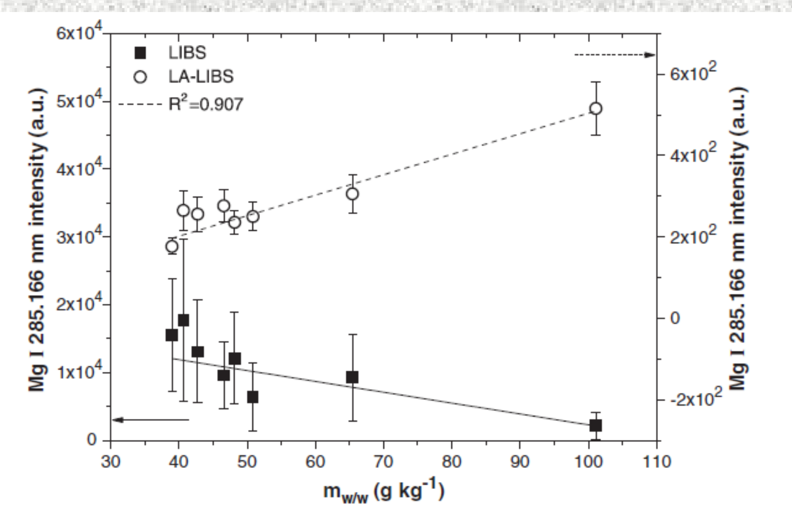

Comparison of LIBS and LA-LIBS calibration curves for Mg in phosphate matrix pellets.

Stepankova, K.; Novotny, K.; Vasinova Galiova, M.; Kanicky, V.; Kaiser, J.; Hahn, D.W., Laser ablation methods for analysis of urinary calculi: Comparison study based on calibration pellets. *Spectrochimica Acta Part B-Atomic Spectroscopy,* 2013, 81, 43-49.

Liquid samples

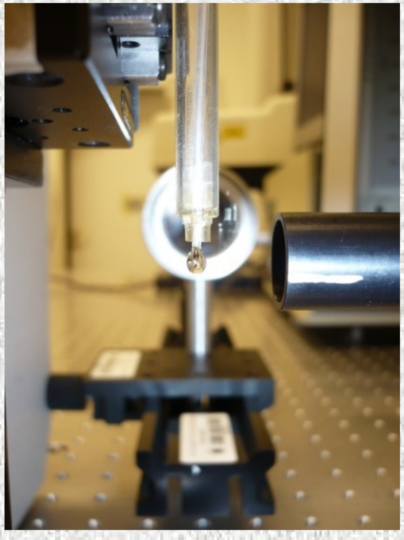

Investigation of liquid samples or bio-fluids (algae suspension)

Instrumentation at Institute of Physical Engineering BUT Brno (prof. J. Kaiser)

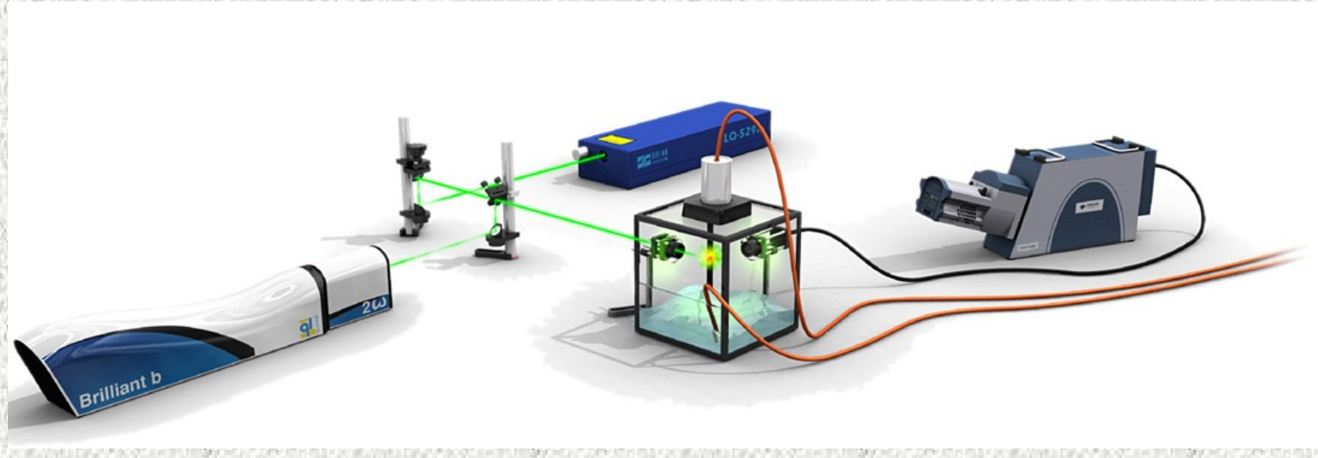

LIBS system employing laminar water jet setup

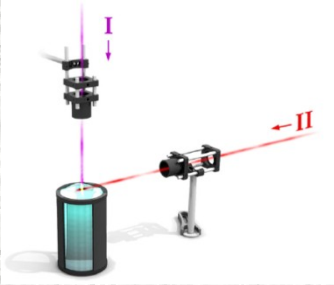

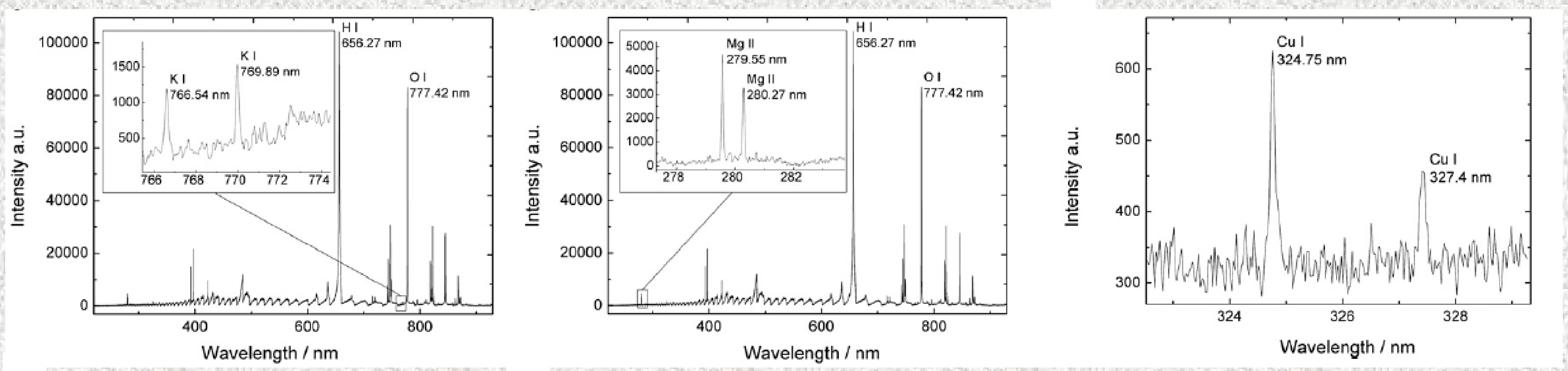

Segments of LIBS spectra of algae suspensions recorded using water jet liquid arrangements

Porizka, P.; Prochazka, D.; Pilat, Z.; Krajcarova, L.; Kaiser, J.; Malina, R.; Novotny, J.; Zemanek, P.; Jezek, J.; Sery, M.; Bernatova, S.; Krzyzanek, V.; Dobranska, K.; Novotny, K.; Trtilek, M.; Samek, O., Application of laser-induced breakdown spectroscopy to the analysis of algal biomass for industrial biotechnology. *Spectrochimica Acta Part B-Atomic Spectroscopy,* 2012, 74-75, 169-176.

Nanoparticles (QDs)

Spatial distribution of quantum dots (QDs)

- cadmium containing QDs – CdS, CdTe
- injection onto the carrier material (chromatographic paper, polystyrene ...)

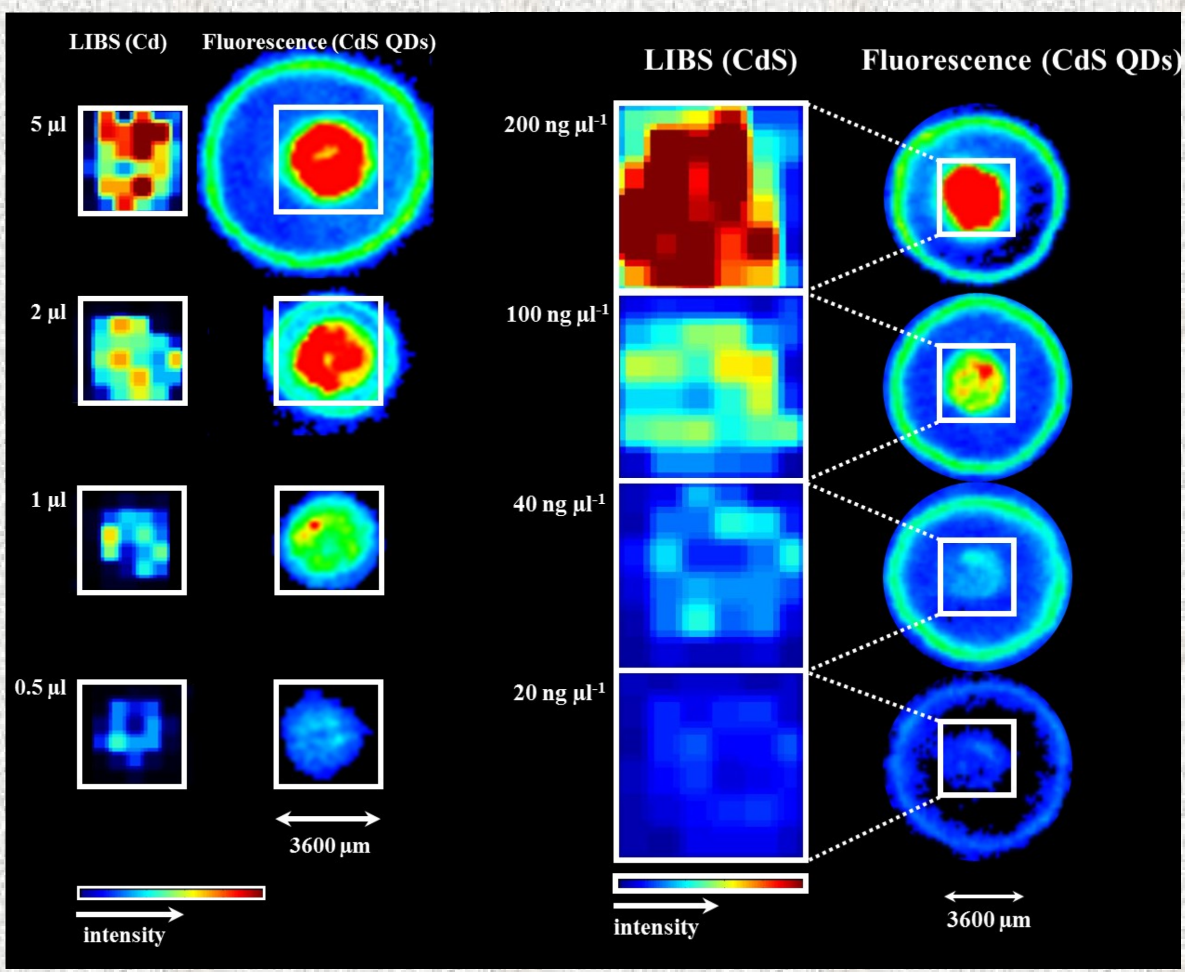

CdS QDs spatial distribution after injection of different volumes and different concentrations on chromatographic paper, 6 x 6 points with spacing 600 µm, emission line Cd (I) 508.58 nm and fluorescence (excitation wavelength 460 nm, emission wavelength 700 nm).

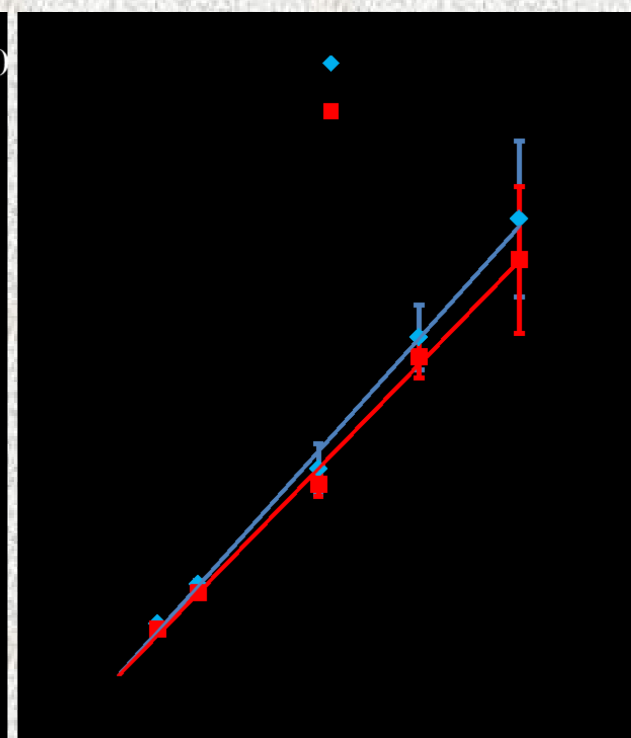

Calibration graphs for injection of 5 µl CdS GSH and CdS MPA solution injected on the chromatographic paper .

Cd signal was obtained by LIBS on emission line Cd(I) 508.58 nm and signal intensity was summarized by counting pixels and all points of raster.

Remote analysis

Stand-off identification of biominerals

Instrumentation developed at Institute of Physical Engineering

BUT Brno (prof. J. Kaiser)

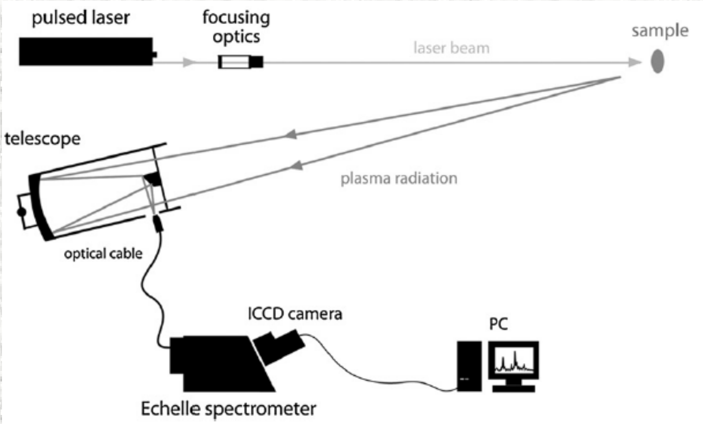

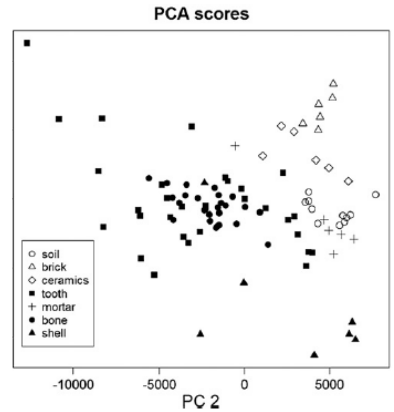

Comparison of linear discriminant analysis (LDA) and artificial neural networks (ANN)
input data - PCA scores

The predictions for test spectra created by LDA (ML) and ANN with back propagation. In the first column there are numbers of test spectra, and in the second one there are real material characters of particular samples. The incorrect predictions are marked in bold.

Test spectrum	Material	LDA (ML)	ANN
No. 11	Soil	Soil	**Ceramics**
No. 12	Brick	Brick	Brick
No. 36	Bear tooth	Bear tooth	Bear tooth
No. 42	mortar	**soil**	mortar
No. 43	Bone	Bone	Bone
No. 50	Shell	Shell	Shell
No. 51	Ceramics	Ceramics	Ceramics
No. 93	Human tooth	**Bone**	Human tooth

List of samples. Training, validation and testing spectra.

Type	Sample	Training spectra	Validation spectra	Testing spectra
Soil pellets	Soil 1	No. 1 No. 2 No. 3 No. 5	No. 4	
	Soil 2	No. 6 No. 7 No. 8 No. 9 No. 10		
	Soil 3			No. 11
Bricks	Brick 1			No. 12
	Brick 2	No. 77 No. 78 No. 79 No. 80	No. 81	
Ceramics	Tile	No. 13 No. 14 No. 15 No. 17	No. 16	
	Green potsherd			No. 51
Mortars	Fine-grained mortar	No. 37 No. 38 No. 39 No. 41	No. 40	
	Coarse-grained mortar			No. 42
Teeth	Bear tooth 1	No. 18 No. 19 No. 21	No. 20	
	Bear tooth 2	No. 22 No. 23 No. 24 No. 25 No. 26 No. 27 No. 28 No. 29 No. 30 No. 31 No. 32 No. 33 No. 35	No. 34	
	Bear tooth 3			No. 36
	Human tooth 1			No. 93
	Human tooth 2	No. 82 No. 83 No. 84 No. 85 No. 87 No. 88 No. 89 No. 90 No. 91 No. 92	No. 86	
Bones	Swine bone			No. 43
	Syphilitic human bone	No. 52 No. 53 No. 54 No. 55 No. 56 No. 57 No. 58 No. 60 No. 61 No. 62 No. 63 No. 64 No. 65 No. 66 No. 67 No. 68 No. 69 No. 71 No. 72 No. 73 No. 74 No. 75 No. 76	No. 59 No. 70	
Shells	White shell	No. 44 No. 45 No. 46 No. 47 No. 49	No. 48	
	Brown shell			No. 50

Vitkova, G.; Novotny, K.; Prokes, L.; Hrdlicka, A.; Kaiser, J.; Novotny, J.; Malina, R.; Prochazka, D., Fast identification of biominerals by means of stand-off laser-induced breakdown spectroscopy using linear discriminant analysis and artificial neural networks. *Spectrochimica Acta Part B-Atomic Spectroscopy* 2012, 73, 1-6.

Conclusion

- rapid progress during the last two decades
- significant improving of LIBS measurement
  (advanced lasers, detection systems and data processing)
- improving precision and accuracy
  (process monitoring, on-line/on-situ screening)
- further improving to be accepted as an analytical technique for quality control
- commercialization
- rapidly expanding field of LIBS applications

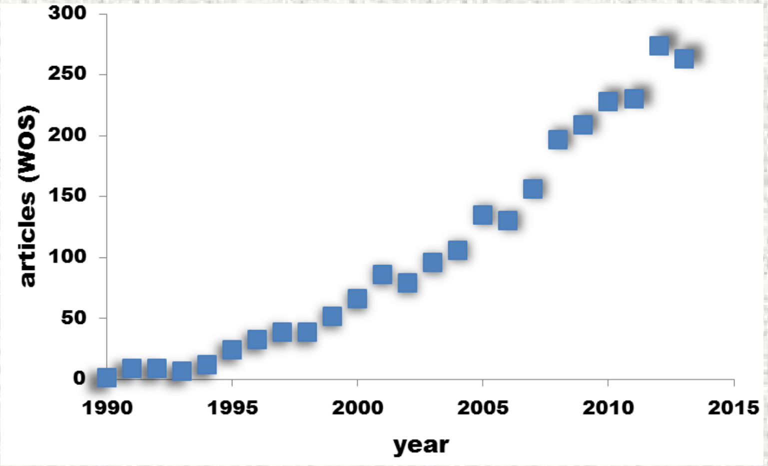

Perspectives at the Department of chemistry PřF MU:

- further development of instrumentation and methodology
- applications on real samples to solve the real scientific problems
- cooperation with the Institute of Physical Engineering BUT Brno, Department of Chemistry and Biochemistry Mendel University in Brno, etc.
- involvement in the project CEITEC
- continuation of international cooperation with many universities and research teams around the world

Self-portrait of *Curiosity* in Gale Crater on the surface of Mars (October 31, 2012)

Radziemski, L. ; Cremers D., A brief history of laser-induced breakdown spectroscopy: From the concept of atoms to LIBS 2012 , *Spectrochimica Acta Part B-Atomic Spectroscopy* 2013, 87, 3-10